Studies on the functional role of HVR domain in the small G-protein H-Ras and its application to Artificial control of Ras

March, 2022
NAHAR RUFIAT (19D5603)

Abbreviation

GTP	Guanosine 5'-triphosphate
GDP	Guanosine 5'-diphosphate
Da	Dalton
DTT	Dithiothreitol
DMF	N,N- dimethylformamide
THF	Tetrahydrofuran
PIPES	Piperazine-1,4-bis (2-ethanesulfonic acid)
EGTA	O,O'- Bis (2-aminoethyl)ethylene-N,N,N',N'- tetra acetic acid
EDTA	Ethylenediamine-N,N,N',N'-tetra acetic acid
TCA	Trichroloacetic acid
Tris	2-Amino-2-(hydroxymethyl) propane-1,3-diol
HEPES	2-4-(2-hydroxyethyl) piperazin-1-yl] ethanesulfonic acid
EDC	1-Ethyl-3-(3-dimethylaminopropyl)carbodiimide
Pi	Phosphate

UV	Ultraviolet
VIS	Visible
SDS-PAGE	Sodium dodecyl sulphate-polyacrylamide gel electrophoresis
PDB	Protein Data bank
SD	Standard deviation
HVR	Hyper Variable Domain
GEF	Guanine Nucleotide Exchange Factor
GAP	GTPase Activating Protein
TEM	Transmission Electron Microscopy
SAXS	Small Angle X-ray Scattering
PAM	4-phenylazophenyl maleimide
NBB	2-Nitrobenzyl bromide

CONTENTS

Chapter 2

Multimerization of small G-protein H-Ras induced by chemical modification at hyper variable region with caged compound

Chapter 3

Photocontrol of GTPase cycle and multimerization of the small G-protein H-Ras using photochromic azobenzene derivatives

List of figures

Chapter 1

Chapter 2

Chapter 3

ABSTRACT

Ras is one of the Small G proteins which is known as a molecular switch, is a central regulator of cellular signal transduction processes leading to transcription, cell cycle progression etc. The active ON state and the inactive OFF state of Ras are regulated by the two factors. GTPase activating protein (GAP) induce hydrolysis of GTP to GDP resulting in formation of inactive state of Ras. On the other hand, Guanine nucleotide exchange factor (GEF) replaces GDP with GTP and make Ras ON state. The switching mechanisms utilizing conformational changes in the nucleotide-binding motifs have been well studied at the molecular level. Interestingly, recent studies have shown that G proteins have a common nucleotide-binding motif with the ATP-driven motors, myosin and kinesin. These nucleotide binding proteins might be evolved from a common nucleotide-binding ancestral protein and share a common catalytic core region including switch I, Switch II and P-loop, and molecular mechanism utilizing a nucleotide hydrolysis cycle . Previously Studies demonstrated that incorporation artificial regulatory nanodevices such as a photochromic molecule into the functional site of Kinesin enable to control ATPase activity photoreversibly . Interestingly, Hyper Variable Region (HVR) is one of the functional parts of the G proteins in which modification induce multimerization and interaction with plasma membrane of Ras. In physiological state Ras forms the nanocluster on the plasma membrane by the lipid modifications of the hypervariable region (HVR) at C-terminal to exhibit physiological function . It is believed that this HVR domain might play a crucial role in Ras protein to its cellular function. First in this study, we have demonstrated that chemical modification of cysteines residues in HVR with caged compounds instead of lipidation induces multimerization of H-Ras. Sulfhydryl-reactive caged compound, 2-Nitrobenzyl bromide (NBB) was stoichiometrically incorporated into the cysteine residue of HVR and induced formation of Ras multimer. Light irradiation induced elimination of

2-Nitrobenzyl group, resulting in conversion of multimer to monomer. SEC-HPLC and Small angle X-ray scattering (SAXS) analysis revealed that the H-Ras forms pentamer. Electron microscopic observation of the multimer showed circular ring shape which is consistent with the structure estimated from X-ray scattering. The shape of the multimer may reflect the physiological structural state of Ras. It was suggested that the multimerization and monomerization of H-Ras was controlled by the modification with caged compound at HVR and light irradiation reversibly. However, caged compound exhibit irreversible photo eliminating reaction. Therefore, caged compounds does not work as a reversible photo-switch. In further study, we employed the azobenzene derivative as a photo reversible nano switching device and incorporated into the HVR to control Ras function.

We introduced the two highly different polarity photochromic sulfhydryl-reactive azobenzene derivatives, 4-phenylazophenyl maleimide (PAM) and 4-chloroacetoamido-4'-sulfo-azobenzene (CASAB) into cysteine residues in HVR to regulate the GTPase activity by photoirradiation. PAM was stoichiometrically incorporated into the three cysteine residues in HVR and induced multimerization. The PAM-modified mutants exhibited reversible alterations in GTPase activity accelerated by GEF And GAP, and multimerization accompanied by photoisomerization upon exposure to ultraviolet and visible light irradiation. CASAB was incorporated into two of the three cysteine residues in HVR but not induced multimerization. GTPase of the H-Ras modified with CASAB was photocontrolled more effectively than PAM-H-Ras. Interestingly CASAB modification did not induced H-Ras multimerization. The results suggest that incorporation of photochromic molecules into its functional site enables photoreversible control of the function of the small G protein Ras. Well known photochromic compounds show light sensitivity at a specific wavelength. Upon light irradiation photochromic compounds can change their structure and

functions. There are two types of mechanisms observed for returning to their original states. A mechanism that returns by irradiating light with a different wavelength, it's called P-type such as diarylethene and fulgide. Another one, a mechanism that returns by heat, it's called T-type such as spiropyran, azobenzene, and stilbenes. In this study we used small caged compound which may mimic the physiological lipidation and photochromic compound such as azobenzene derivatives. We employed a sulfhydryl group reactive caged compound to modify the cysteine residues in HVR. NBB used in this study is one of the well-known cage compounds and can be specifically introduced into the thiol group of the cysteine residue as shown in Then, by light irradiation at 340-400 nm, the nitrobenzyl group is eliminated and the protein reversibly returns to its original state. There are 6 cysteine residues in Human H-Ras. Three of them are in the globular domain and C118 is located on the surface. The remaining three cysteine (C181, C184,C186) which are known as lipidation sites are in the HVR domain. HVR domain is exposed to solvent. NBB is incorporated in to the cysteine residues stoichiometrically. Therefore, it is assumed that the four cysteine residues (C118, C181, C184 and C186) exposed to solvent are modified specifically.

CHAPTER 1

INTRODUCTION

G-protein:

Guanine nucleotide-binding protein, also known as G proteins, this family of proteins categorized as a molecular switches from external to internal signal transmission by responding to a variety of external responses. By the regulatory factors it can control its ability to attach to and convert GTP (guanosine triphosphate) to GDP (guanosine diphosphate) by hydrolysis. Physiologically GTP bound state is considered as an 'on' state whereas its 'off' state is when it binds with GDP. Guanine nucleotide-binding protein is a part of a large group of enzymes named GTPase. The classification of G-protein is as follows: one of them is small G-protein which is also known as small GTPase and the latter one is G-protein heteromeric complex (1-5). Heteromeric G-protein complex is composed of alpha (α), beta (β) and gamma (γ) subunits. Additionally, a stable dimer referred to as beta-gamma complex was found physiologically which is made of beta and gamma subunit. With the molecular weight of 20-25kDa the small G-protein is considered as Ras superfamily of small GTPase. These small G-proteins are similar to alpha subunits of heteromeric G-proteins although they are monomeric and hold only one unit. Large number of G-proteins are found in eukaryotic cells which are involved in the signal transmission pathway. For example, In human gene 18 types of Gα , 5 types of Gβ and about 12 types of Gγ proteins have been found (Fig 1-4). The ATP-binding proteins and the G motif of G-protein share common structure such as nucleotide binding domains (Switch I, Switch II, P-loop). The most stable and indissociable dimer is Gβ complex where Gγ binds to the N-terminal, specifically at the coiled coil region and the external part of the β-propeller of the Gβ structure. Moreover, attached to the cell membranes, G-proteins modify the Gα and Gγ with lipids. In response to the external stimuli the dissociation of Gα GDP occurred and allows GTP to bind to the on state of G-protein (5-7). As a result the information transferred by the dispatch of Gα and Gβγ and the target protein can bind to the Gα subunit. To

return to the off state of the protein hydrolysis of GTP is required and in return the complex of Gα and Gβγ associates. Different function played by heteromeric G-

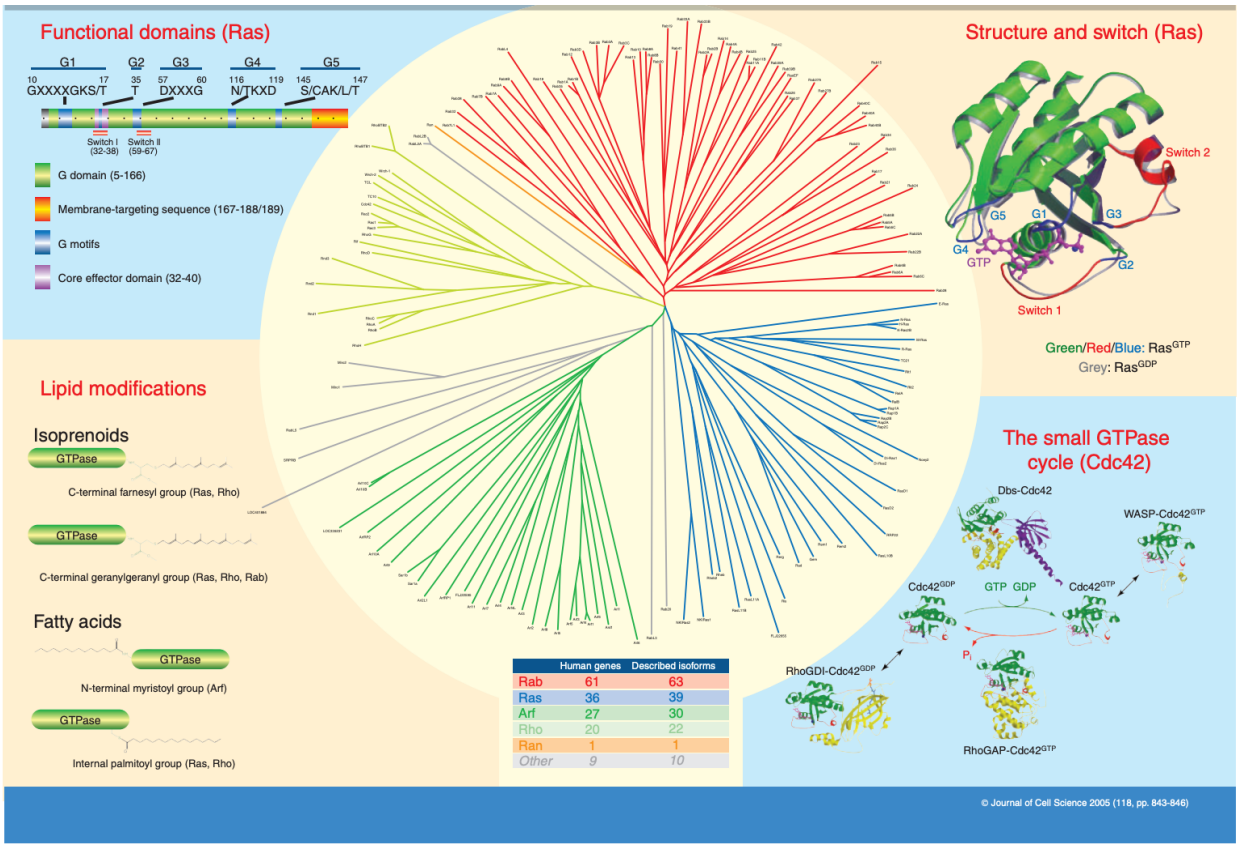

Fig 1: Ras superfamily (Journal of Cell Science 118, 843-846 Published by The Company of Biologists 2005 doi:10.1242/jcs.01660)

protein for example regulation of adenylate cyclase was done by Gs and Gi where Gs accelerated the function conversely and Gi induces the inhibition activity. In addition Gq controls the function of phospholipase C.

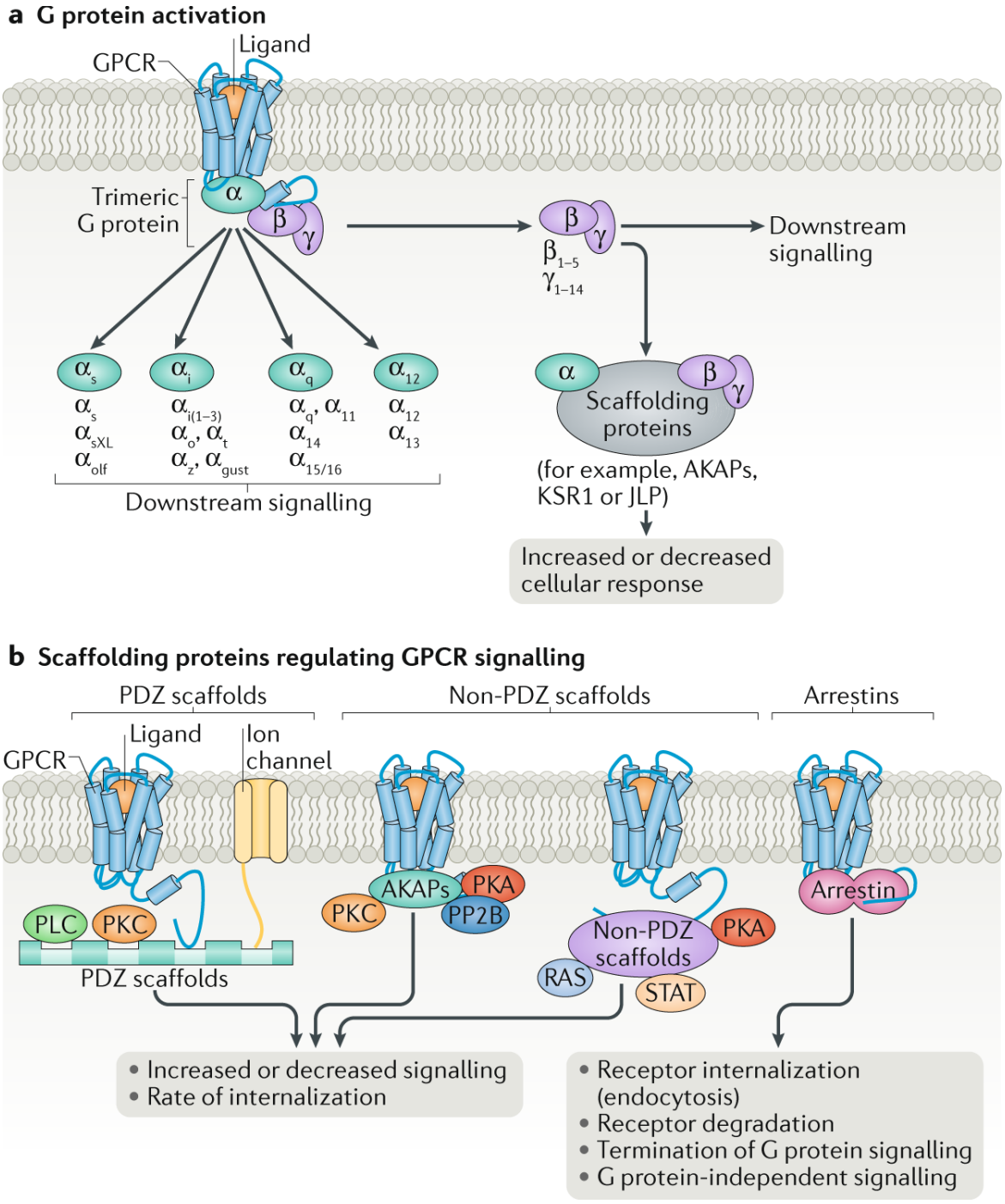

Fig 2: Schematic illustration of GPCR signalling.
(Nature Reviews Molecular Cell Biology (Nat Rev Mol Cell Biol)

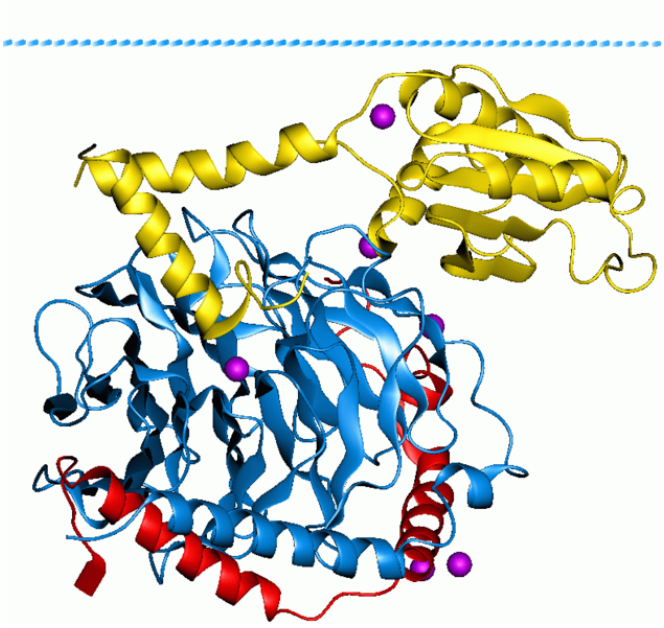

Fig 3: Phosducin- transducin beta-gamma complex. Beta and gamma subunits of G-protein are shown by blue and red, respectively.
(https://www.wikiwand.com/en/G_protein#/google_vignette)

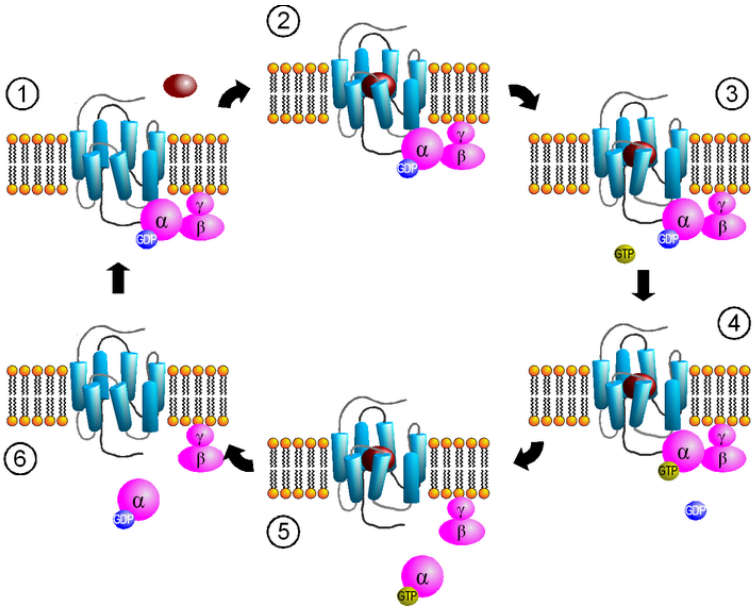

Fig 4 : Activation cycle of G-proteins (pink) by a G-protein-coupled receptor (GPCR, light blue) receiving a ligand (red). (Stewart, Adele; Fisher, Rory A. (2015). Progress in Molecular Biology and Translational Science. 133. Elsevier. pp. 1–11.)

Small G-protein :

Small GTPase has typically 20-25kDa molecular weight which can interchange its active, GTP-bound conformation and inactive state, GDP-bound conformation. Ras is the founding member of all Small G-proteins, responsible for 15% of all human cancer due its point mutation. The group of 154 members of the human Ras superfamily is classified into final five major classes such as Ras, Rho, Rab, Arf, and Ran which are functionally and structurally conserved membrane proteins from yeast cell to mammal cell (8-12) (Fig 5-6). The cysteine residues in the Hyper variable domain (HVR) of Ras directly attach to the plasma membrane by lipidation. Ras proteins control various intra cellular processes. For instance, Ran G-protein transports nuclear and helps in the formation of nuclear envelope and therefore controls spindle preparation.

The Ras superfamily of small GTPases

Family	Subfamily	Function	Members
Ras	Ras	Cell proliferation, differentiation, survival, apoptosis, gene expression	E-Ras; N-Ras; H-Ras; K-Ras; M-Ras; R-Ras; R-Ras2; Di-Ras1; Di-Ras2; Di-Ras3; NKIRas1; NKIRas2; RasD1; RasD2; RasL10A; RasL10B; RasL11A; RasL11B; RasL12, Rerg
	Ral	GTP-dependent exocytosis	RalA, RalB
	Rap	Cell–cell and cell–matrix adhesion	Rap1A; Rap1B; Rap2A; Rap2B; Rap2C
	Rad	Cell shape remodelling, cell-cycle checkpoint	Rad, Gem, Kir, Rem1, Rem2
	Rheb	mTOR pathway, cell growth and cell-cycle progression	Rheb; RhebL1
	Rit	Neuronal differentiation and survival	Rit1; Rit2; Rin; Ric
Rho		Cytoskeletal dynamics; cell shape, polarity, adhesion, and movement; cell-cycle progression; gene expression	RhoA; RhoB; RhoBTB1; RhoBTB2; RhoBTB3; RhoC; RhoD; RhoF; RhoG; RhoH; RhoJ; RhoQ; RhoU; RhoV; Rnd1; Rnd2; Rnd3; Rac1; Rac2; Rac3; Cdc42
Rab		Membrane and protein traffic in the endocytic and secretory pathways	Rab1A; Rab1B; Rab2; Rab3A; Rab3B; Rab3C; Rab3D; Rab4A; Rab4B; Rab5A; Rab5B; Rab5C; Rab6A; Rab6B; Rab6C; Rab7A; Rab7B; Rab7L1; Rab8A; Rab8B; Rab9; Rab9B; RabL2A; RabL2B; RabL4; Rab10; Rab11A; Rab11B; Rab12; Rab13; Rab14; Rab15; Rab17; Rab18; Rab19; Rab20; Rab21; Rab22A; others
Arf		Vesicular trafficking, endocytosis, and exocytosis	Arf1; Arf3; Arf4; Arf5; Arf6; Arl1; Arl2; Arl3; Arl4; Arl5; Arl5C; Arl6; Arl7; Arl8; Arl9; Arl10A; Arl10B; Arl10C; Arl11; Arl13A; Arl13B; Arl14; Arl15; Arl16; Arl17; TRIM23, Arl4D; ArfRP1; Arl13B
Ran		Nucleocytoplasmic transport; mitotic spindle organization	Ran

Fig 5 : Small G-protein classification
(The Ras Superfamily of Small GTPases: The Unlocked Secrets.DOI: https://www.researchgate.net/publication/259956774)

Other members such as Rab (30 members) and Arf (6 types) possess vesicle related activity starting from vesicle formation and transportation to the exocytosis. On the other hand, controlling the cell migration, morphology and cytoskeleton, main functions of Rho family members named Rho, Cdc42 and Rac. Importantly, cellular signal transduction , cell transcription, differentiation and proliferation are regulated by small G-protein Ras (13).

Fig 6 : HRas structure PDB 121p, surface colored by conservation in Pfam seed alignment: gold, most conserved; dark cyan, least conserved.

The GDP to GTP exchange is highly controlled by one of the regulator GEFs which helps to remove the bound GDP in response to more abundant guanine triphosphate (GTP) whereas GAPs promotes an essential catalytic part to hydrolyze the GTP. By lipid modification (such as farnesyl and geranylgeranyl) at the C terminus of small G-protein, which helps the small G-protein to localize to the plasma membrane and promotes lipid anchoring. One possible approach to control a subset of Rab and Rho families of Small G Protein is to target the nucleotide dissociation through inhibitors (14-15). Ras superfamily which is directly involved in the cancer formation due to frequent mutation can be controlled by targeting the GTPase cycle, nanocluster formation and regulatory factor inhibition.

Ras and their superfamily:

Ras protein is named after a rat of sarcoma since it was found from the acroama. Ras proteins regulate cellular signal processes found in 30% of all human malignant formation and focused on potent techniques for cancer regulation (Fig 7). Frequent point mutation is confirmed in tumor cells in Ras protein. Three different types of Ras protein include sarcoma-derived H-Ras discovered by Jennifer Harvey in the 1960s, sarcoma-derived K-Ras discovered by Kirsten Werner, and N- invented in human neuroblastoma cells.

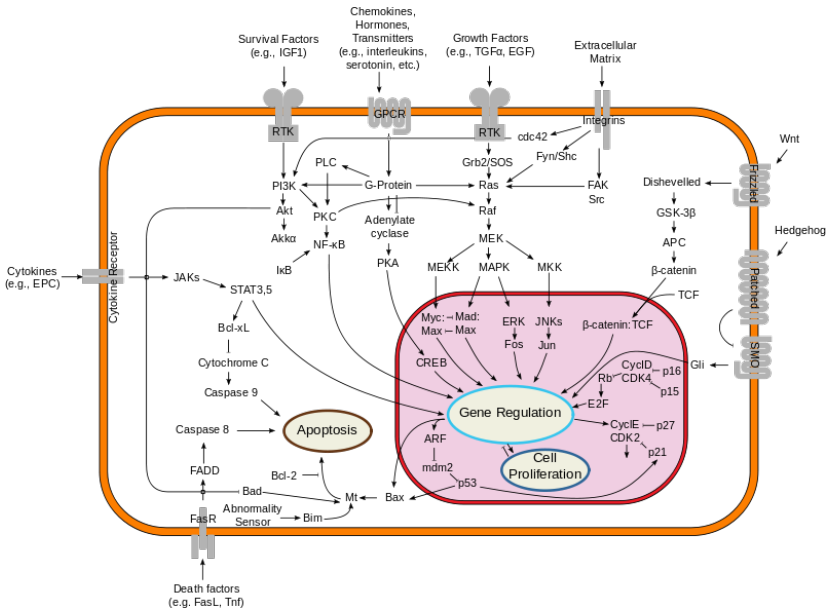

Fig 7 : Signal transduction pathways

(https://commons.wikimedia.org/wiki/File:Signal_transduction_pathways.svg)

Ras is roughly 21 kDa in size with 188-189 amino acids and has a site for binding GTP or GDP as well as an effector loop for interacting with PI3 kinase (PI3K), Raf, and Ral-GEF (Fig 8-9). Ras contains a single β-sheet consisting of 5 α-helices and 6 β-strands . Operative domains on the primary structure include nucleotide binding-related domains G1 motif Ploop: 10-16 amino acids (GXXXGK (S / T), motif G2 which is Switch I amino acid number 30-40 (XTX), Switch II which

is G3 domain from 60-76aa (DXXGXE), G4 from 116-119aa (NKXD), G5 domain: 143-147aa (EXSAX) and effector interaction domain exists.

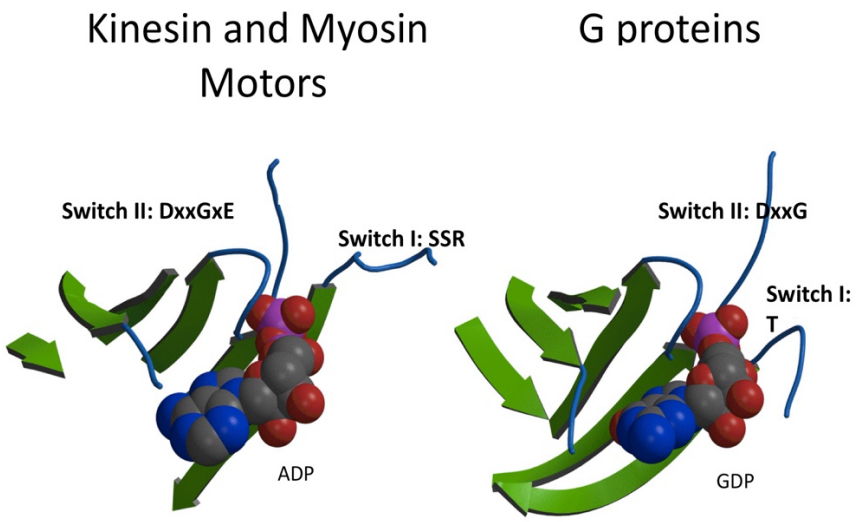

Fig 8: The nucleotide binding pocket of kinesin, myosin, and G proteins displays a similar architecture consisting of 5 parallel beta-strands and one anti-parallel strand. Four loops emerge from these strands to contact the nucleotide, two of which (switch I and switch II) are involved in contacting the gamma-phosphate and relaying structural changes in the protein that alter interactions with other proteins (e.g. polymers or other binding partners) and conformational changes that produce force.
Vale, Ronald D. (1996) Switches, latches and amplifier: common themes of G proteins and molecular motors (Commentary). J Cell Biol 135: 291-302).

Switch 1 and 2 play different roles in nucleotide binding in small GTPases (16-20). Switch I undergoes complex formation with the base and the sugar moiety of the guanine of GDP and GTP in case of Rab, Rho and Ras G proteins, whereas other Ras proteins such as Ran , Arf remains far from the guanine diphosphate and a significant conformational change go through when binds to GTP nucleotide. Additionally, the switch I region of all active state GTPase provides a conserved threonine to interact with the Mg2+ and the γ-phosphate of GTP. On the other hand, by the invariant DTAGQ/T/H motif of the switch II react with the γ-phosphate of GTP with the help of glycine residue.

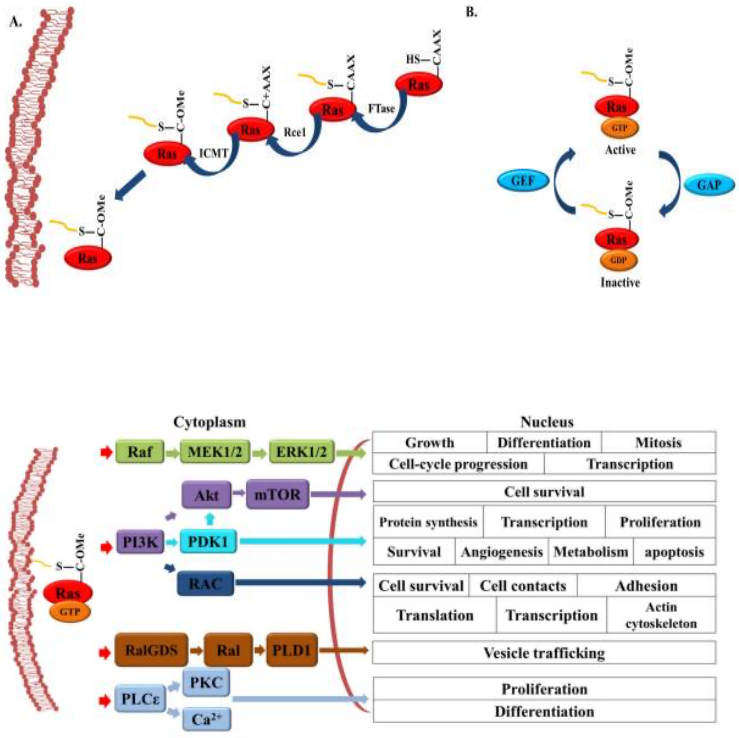

Fig 9: Regulation of Ras membrane association and Regulating signaling downstream of Ras. (Han, C. W., Jeong, M. S., & Jang, S. B. (2017). Structure, signaling and the drug discovery of the Ras oncogene protein. BMB reports, 50(7), 355–360. https://doi.org/10.5483/bmbrep.2017.50.7.062)

Interestingly, glutamine of this region plays a crucial role to catalyze the GTP hydrolysis in the presence of GAP which is specific for Ras and other small GTPase. Furthermore, cysteine residues in the Hypervariable Region (HVR) is a membrane protein that is lipid modified and can bind to the cell membrane (Fig10-11). In the endoplasmic reticulum, all C186s in the Ras family tends to irreversible farnesyl lipid modification, and removing the AAX component of the CAAX motif methylates the farnesyl-linked cysteine. In addition H-Ras, N-Ras, and K-Ras4A all have Cysteine 181 and Cysteine 184 which also follows reversible palmytoilation in the Golgi apparatus and depalmytoilation in the plasma membrane. Oncogenic point mutations have been found in vivo at

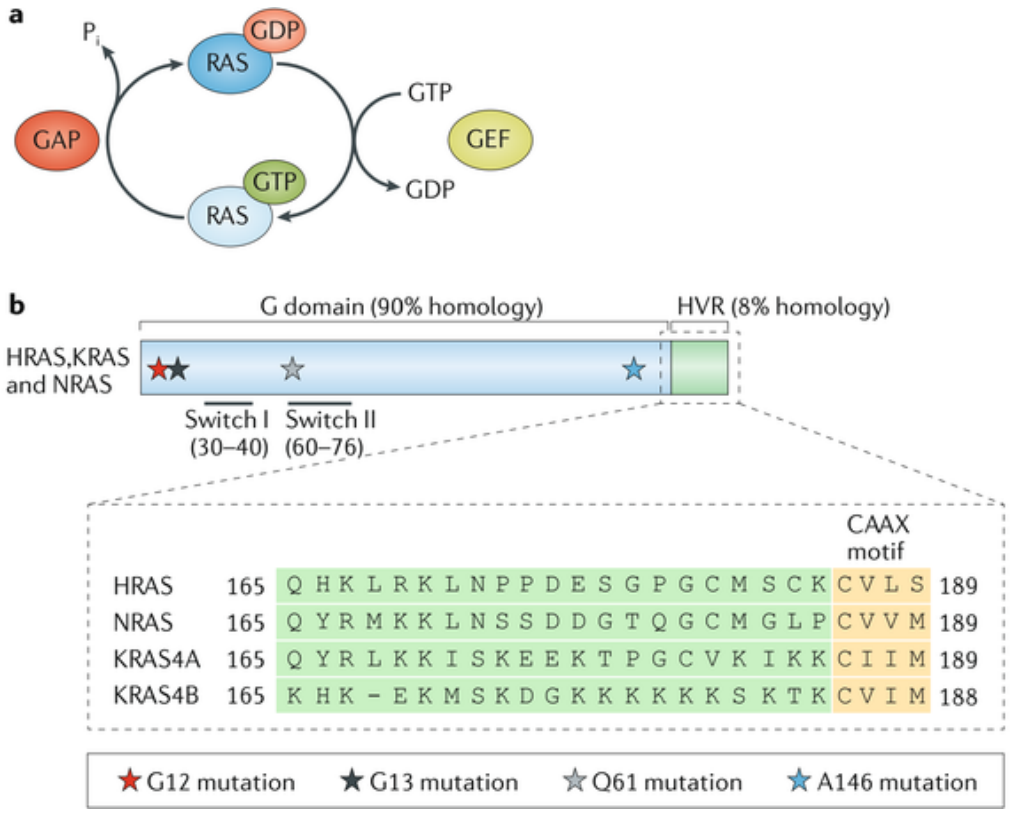

Fig 10: Sequence of H-Ras, K-Ras and N-Ras
(Simanshu, D. K., Nissley, D. V., & McCormick, F. (2017). RAS Proteins and Their Regulators in Human Disease. Cell, 170(1), 17–33. https://doi.org/10.1016/j.cell.2017.06.009)

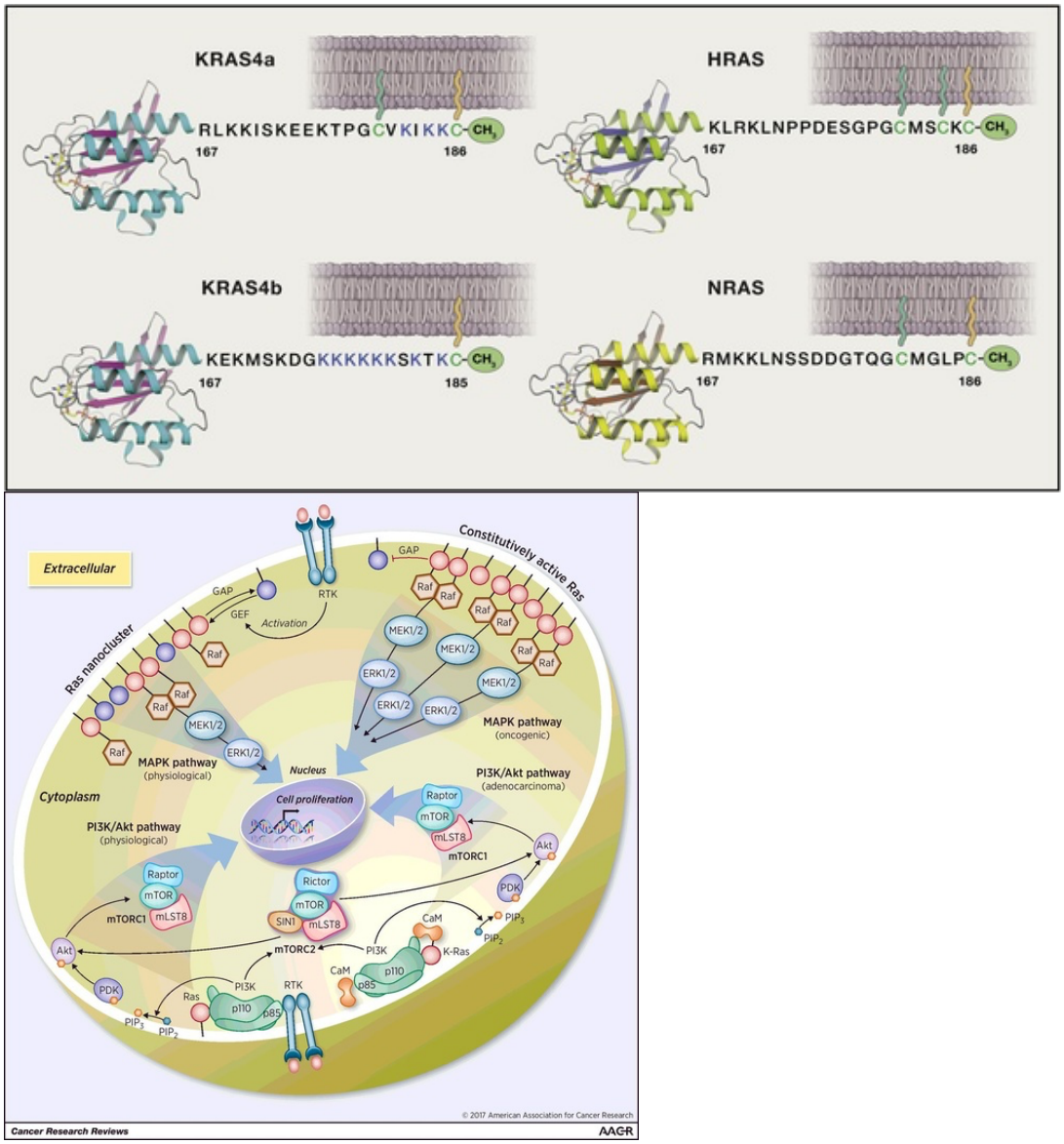

Fig 11: Lipid anchoring of Ras protein and physiological pathways. (https://cancerres.aacrjournals.org/content/78/3/593)

exons 12, 13, and 61aa with each RAS isoform resulting in one of 19 potential point mutations. RAS mutations stop the GTPase from working and keep the protein in on state which is GTP bound condition. Due to the mutation in Ki specific Ras gene, which is reported to have critical function in the mutagenesis of human cancer formation, 95% pancreatic cancer was found, the percentage of colon cancer is 50 and 30% of lung tumorigenesis (21-25). Ras activates a number

of pathways, the most well-known of which is the mitogen-activated protein (MAP) kinase cascade. This cascade transfer signals downstream, causing genes involved in cell growth and division to be transcript. The PI3K/AKT/mTOR pathway, which increases protein synthesis and cellular proliferation while inhibiting apoptosis, is another Ras-activated signaling system.

Motor proteins:

Myosin is a cytoskeleton-associated protein that is involved in muscle contractionwhich acts a biomolecular machine and utilizes kinetic energy by hydrolyzing ATP with the help of actin filament having a fibrous structure such as rails. Myosin consisting two heavy chains (HC, 229 kDa), RLC, a regular lightchain (20 kDa), and an ELC (Essential light chain:17 kDa). A large superfamily of genes of myosin produce a protein which has essential characteristics to bind with the actin and can hydrolyze ATP for force transmission which is also known as an ATPase enzyme activity. All Myosin proteins are composed of a head, a neck region and a tail-like domain. Usually, the head region of myosin protein attaches to the actin filament and catalyzes ATP hydrolysis to generate force and move forward to the barbed (+) end along the filament. Whereas myosin VI walks exceptionally to the negative (-) end of the actin filament. The neck domain of myosin functions as a linker and liver-like arm to convey the energy force from the catalytic domain to the remaining body (26). In addition, the light chain of the myosin binds to the neck domain whichprovides a part to interact with distinct proteins to form a macromolecular complex, functioning as a regulator. In general, other myosin subunits and/or cargo molecules form a complex with the tail part. It is reported that, the tail domain of myosin plays an important role to regulate the motor activity (27). The troponin-tropomyosin complex regulatesskeletal muscle contraction on the actin side Fig 12-13 , whereas (MLCK) or myosin lightchain kinase and alkaline

phosphate regulate smooth like muscle contraction inthe myosin head. The process is carried out by

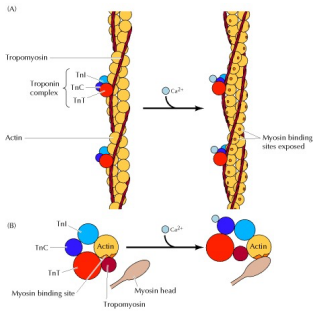

Fig 12: Association of tropomyosin and troponins with actin filaments. (Cooper GM. The Cell: A Molecular Approach. 2nd edition. Sunderland (MA): Sinauer Associates; 2000. Actin, Myosin, and Cell Movement. Available from: https://www.ncbi.nlm.nih.gov/books/NBK9961)

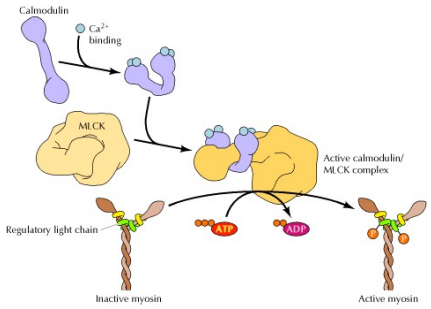

Fig 13: Regulation of myosin by phosphorylation. Ca2+ binds to calmodulin, which in turn binds to myosin light-chain kinase (MLCK). (Cooper GM. The Cell: A Molecular Approach. 2nd edition. Sunderland (MA): Sinauer Associates; 2000. Actin, Myosin, and Cell Movement. Available from: https://www.ncbi.nlm.nih.gov/books/NBK9961)

phosphorylating and dephosphorylating a specific RLC . Phospholipase C is activated when an agonist attaches to a G protein-coupled receptor, and phosphofatidyl inositolde composes inositol trisphosphate (IP3) and diacylglycerol (DAG). Ca2 + isreleased when IP3 interacts to the IP3

receptor in the reticulum of endoplasm, and Ca2 + and calmodulin (CaM) combine to activate MLCK. Activated MLCK phosphorylates RLC, causing structural changes in RLC that allow the smooth muscle myosin head to engage with actin (28) . Because this myosin V functions with a single molecule rather than numerous molecules like myosin II, single molecule research is being actively pursued, such as single molecule motility measurement with a whole internal reflection microscope and single molecule force measurement with optics.

RAS Regulators:

The release of GDP by the combined work of GTPase/nucleotide connections, is a time-consumed process that can be fastened by GEFs in-vivo regulations. Till now, the multistep kinetic reaction of GEF-stimulated nucleotide exchange has been explained for GEF-stimulated nucleotide exchange. At the beginning, the GDP-bound small G protein and the GEF form low-affinity complex between them that turns into a nucleotide-free high-affinity GTPase/GEF molecule after the GDP dispatch (29-35). Then the GTPase become active through the displacement of GEF by GTP binding. In recent studies, the crystallographic structures of GTPase/GEF no nucleotide state complexes have been achieved by removing this attached nucleotide and forming the stable complex. The method of inducing acidic amino acids in the GEFs phosphate-interaction site, results repulsive electrostatic reaction which in turn, releases the attached nucleotide. Another approach is the modification of the Switch II region to direct the methyl group of alanine to the Mg2+-binding site. This cause either alone or combined hydrophobic repulsion (Fig 14-15).

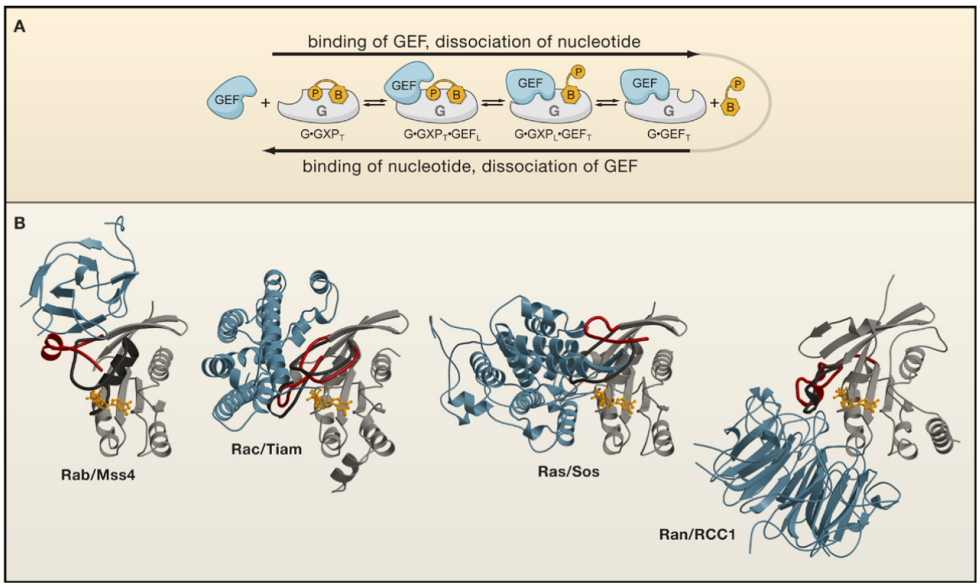

Fig 14: Mechanism of GEF-Induced Nucleotide Exchange
(Cell 129, June 1, 2007 ©2007 Elsevier Inc.)

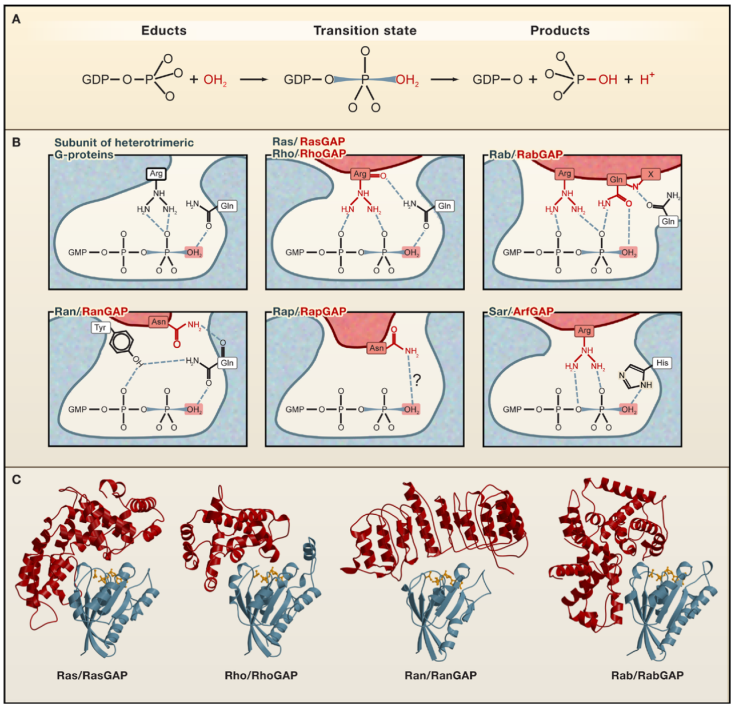

Fig 15: Mechanism of GAP-Induced GTP Hydrolysis
(Cell 129, June 1, 2007 ©2007 Elsevier Inc.)

Depending on these approach, there are multiple ways the GEFs can regulate. For example,

Totally blocking the nucleotide-binding region or partially blocking the Mg2+- or phosphate-

binding regions or sometimes even leaving the nucleotide-binding site without any modification. Although the detailed molecular reason behind this is obscure, it is hypothesized that the crystal capturing discrete intermediates are behind this. The reaction between the lysine from the P-loop with the acidic residues from Switch II cis or GEF trans is connected to the N-terminal REM (Ras Exchanger Motif) domain, activate Ras, Rap, and Ral proteins. In the Fig. 16-17, it has been

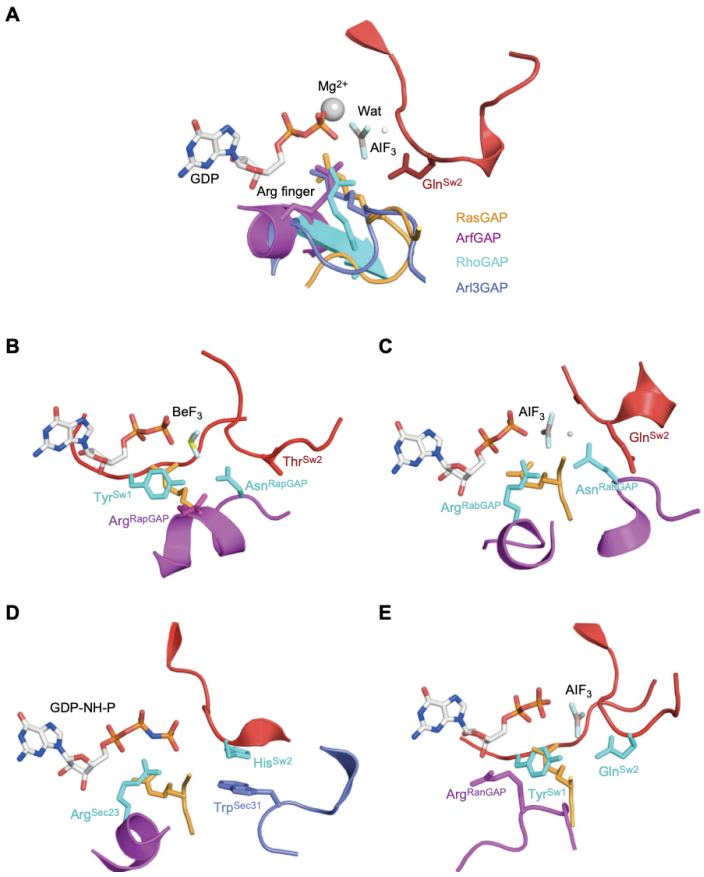

Fig 16: The mechanisms of GAP-stimulated GTP hydrolysis (Physiol Rev 93: 269 –309, 2013 doi:10.1152/physrev.00003.2012)

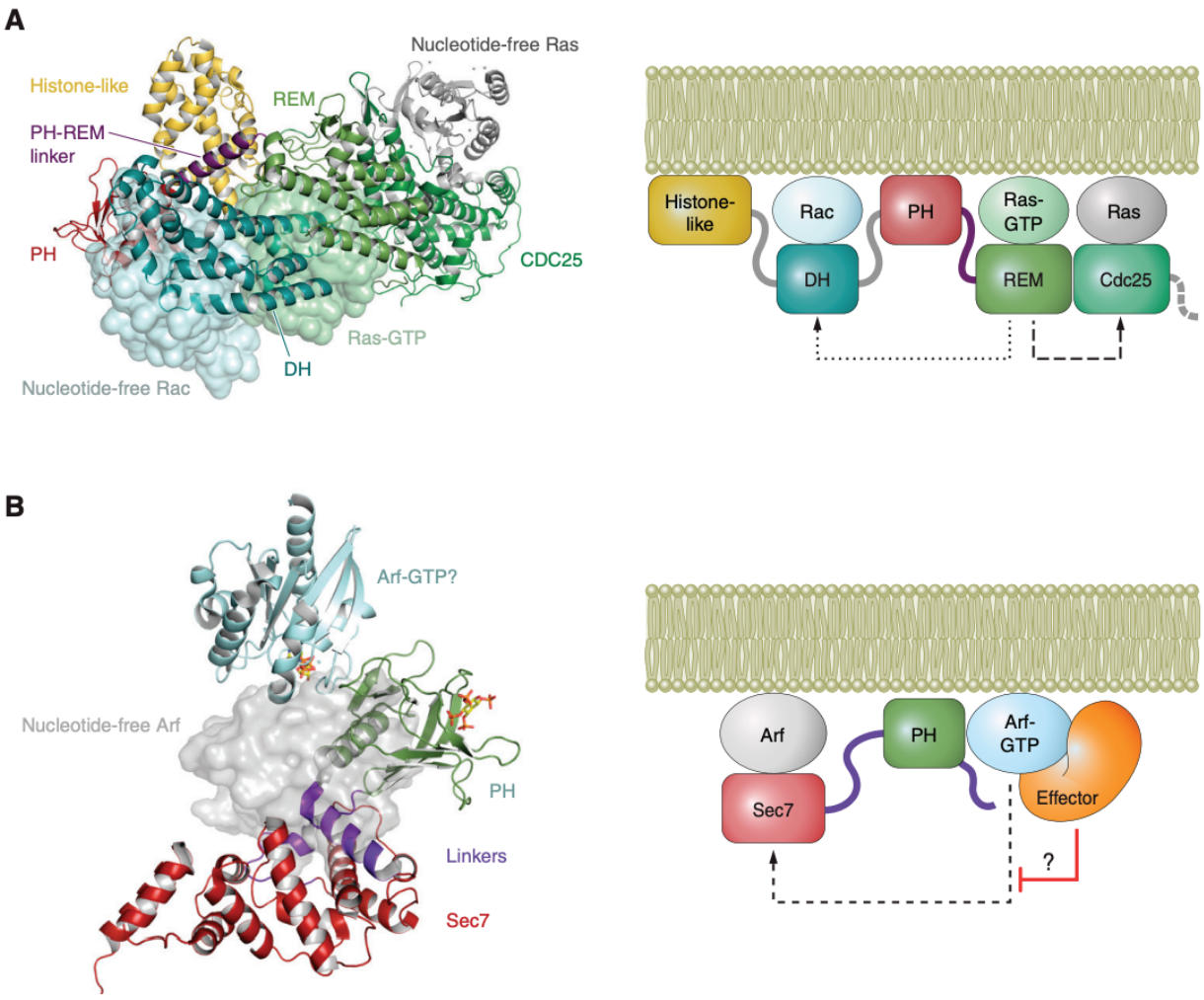

Fig 17: Regulation of GEFs by feedback loops. (Physiol Rev 93: 269 –309, 2013 doi:10.1152/physrev.00003.2012)

demonstrated that the α-helical bowl-like Cdc25 region contains the GTPase-binding site and it made possible because of the crystal structures of the no nucleotide REM-Cdc25 tandems for the Ras specific GEF SOS and the Rap specific GEF EPAC. Due to this, in Ras GRF1 or RalGPS1a, the Cdc25 region can fold itself which is required for nucleotide exchange reaction. It has been clear that, the remodeling of the switch 2 region makes the dissociation of the nucleotide possible

since it redirects Ala59 close to the Mg2+-binding pocket. It also repositions the Glutamine 62 to form and stabilize a salt bridge between the lysine from the P-loop. It has also been revealed in all of the structures that the REM domain can build a close-pocket contact with it regardless of the linking of the CDC25 domain to the associated GTPase. Even though there is no direct contact with the GTPase, an allosteric region for SOS Ras-GTP and the binding domain in the interface for cAMP, EPAC's allosteric inducer are still present. The relatively slow GTPase reactions of the small GTPase are not always relied to the time frame of their cell-regulate activities. Instead, they are dependent on the GAP action based on the demand of the cellular functions. Through the incorporation of aluminum and beryllium fluorides, Chabre discovered that, the transition states can be mimicked which allowed him to have an insight in the GTP hydrolysis steps (36). The target protein either has a GAP or not can be determined by forming a stable GTPase and GAP complex with the addition of Guanine Diphosphate and AlFx. The 3-D structures for all the well-recognized small GTPase/GAP complexes has been identified by adding AlFx or BeF3 and MGF3 with GDP. Through these structures, the molecular mechanism of GAP by which it becomes activated small GTPase, has been cleared. The studies were first carried out for Ras specific GAP domain of GAP (p120) combined with Ras-GDP state AlF4 and the GAP (Rho) region of p50GAP for Rho combined with RhoA in the GDPstate-AlF4. It has been figured out that the arginine finger can be used by GAP to stabilize partially the negative charges that has been produced during the transition state. The formation of the catalytic active site has been possible by positioning the switch 2 glutamine that causes a nucleophilic attack of the GTP phosphate. By this mechanism, the access of the RasGAP arginine finger has been blocked and could be the possible explanation for describing the biochemical problems of the cancer cells due to the RAS mutation, specifically in P-loop (G12V and G13D). Although stabilizing the transition state while forming

tandem of residues to activate the nucleophilic water is the sole mechanism by which GAP works, the switch 2 glutamine or arginine finger has not been used by all GAPs. While trying to develop biochemical tools and doing cellular assays and techniques, these factors and differences need to be considered. Some examples might be the QGAP, which has a Ras specific GAP domain where the arg-finger is altered by the threonine and the inactive RhoGAP region of OCRL, where this arginine has been changed to a glutamine.

Purpose of the study:

The aim of this study is to analysis the Ras nanocluster where HVR domain is involved and control Ras function by utilizing a potent photochromic nanodevices. Multimerization is essential for cell signal transmission. Lipidation of cysteine residues in HVR induces the localization of Ras to the plasma membrane and the formation of multimers. However, the structural basis of multimers related to physiological function has not been clarified because physiological conditions are difficult to study. In this study, we utilized the chemical modification of cysteine residues in HVR by a caged compound, NBB, instead of physiological lipidation, induces the formation of a stable multimer of H- Ras. The removal of caged compounds by light irradiation converts multimers to monomers. Notably, the pentamer model of the NBB-H-Ras multimer estimated from the X-ray scattering analysis and electron microscopic observation showed high similarity with one of the structural models of a pentameric K-Ras nanocluster observed in an in silico study (37). A unique symmetrical pentagonal ring shape was observed among the structures estimated from these analyses. The artificial multimer induced by chemical modification may mimic the physiological nanocluster of Ras in vitro.

Additionally, In this study a potent photochromic nanodevices was developed to photocontrol the Ras GTPase function which is important to provide the physiological function. Ras acts as a molecular switches by GTP hydrolysis. Previously Dr. Iwata, et. al. photocontrolled the Ras GTPase activity by targeting the catalytic part of Ras protein. However incorporating the catalytic part of the Ras protein was not efficient. Therefore, a new idea to photocontrol the RAS GTPase activity was established targeting the core regulatory part of RAS named HVR domain. HVR domain is involved in diverse physiological function such as anchoring at the plasma membrane, isoform specific protein- downstream effector binding and providing high-fidelity signal transmission. Two different polarity azobenzene derivatives was synthesized and incorporated into the HVR domain and successful photoregulation was achieved.

Photochromic compound as a nanodevice:

Different approaches have been taken to control Ras function to overcome cancer formation. Finding and designing of potent inhibitors to target Ras has been identified. However most of the inhibitors showed irreversible regulation and structural varieties. Therefore these cannot be act as a significant nanodevices to achieve the functional regulation. As a result photoswitchable nanodevices can be a good candidate to regulate the Ras function reversibly. To achieve the goal I focused on Chromism compound where the color of the molecule changes reversibly according to the chemical reaction. Some well-known examples of chromism molecules such as pH, heat, light and so on (Fig 18-19). According to the heat or various temperature can shift the structure and properties of thermochromic molecules. Another important chromic molecule is photochromic compound which can change it isomerization upon different light irradiation for a specific period

of time. Cis and trans isomerization However biomolecules such as proteins which is highly sensitive to

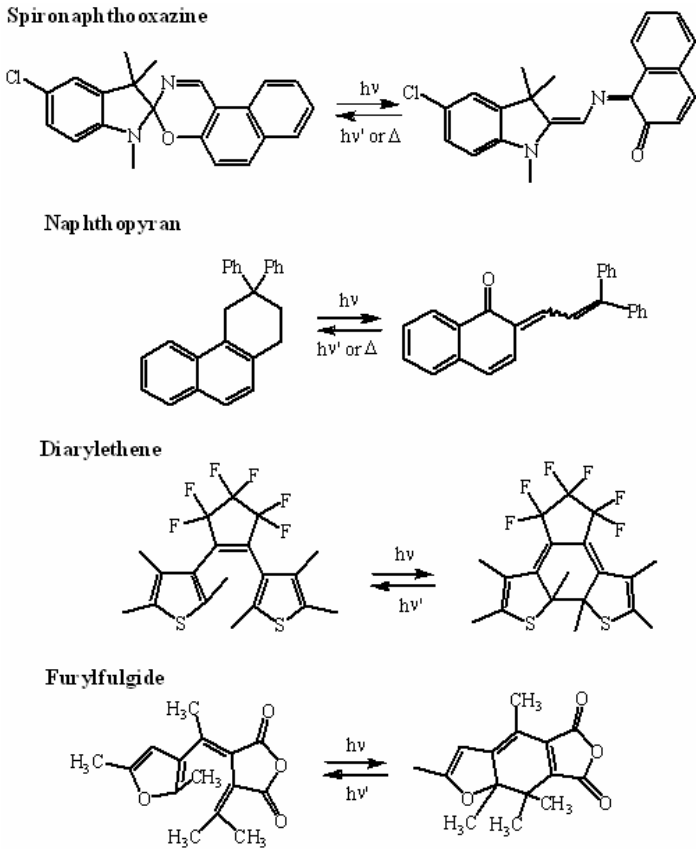

Fig 18: Structural formula of the typical Photochromic compounds
(https://www.researchgate.net/publication/47715122_TWO-PHOTON_3D_OPTICAL_DATA_STORAGE_VIA_FLUORESCENCE_MODULATION_OF_FLUORENE_DYES_BY_PHOTOCHROMIC_DIARYLETHENES)

heat and different pH which can effect protein structure. Therefore in my research I applied photochromic compound which I can utilize according to the light.

Photochromic molecules reported as an efficient nanodevices. UV and Visible light irradiation at a specific wavelength can change the cis and trans isomerization and properties of the compound such as hydrophobic and hydrophilic which can act as a molecular switches. Two categories of

photochromic compound named as P-type and T-type. Photochemically reversible type (P-type) cannot return to its initial structure if temperature is elevated for example: fulgides and diarylethenes and the latter one can convert to its original form upon thermal changes (T-type) such as stilbenes, azobenzenes, or spiropyranes (38-39).

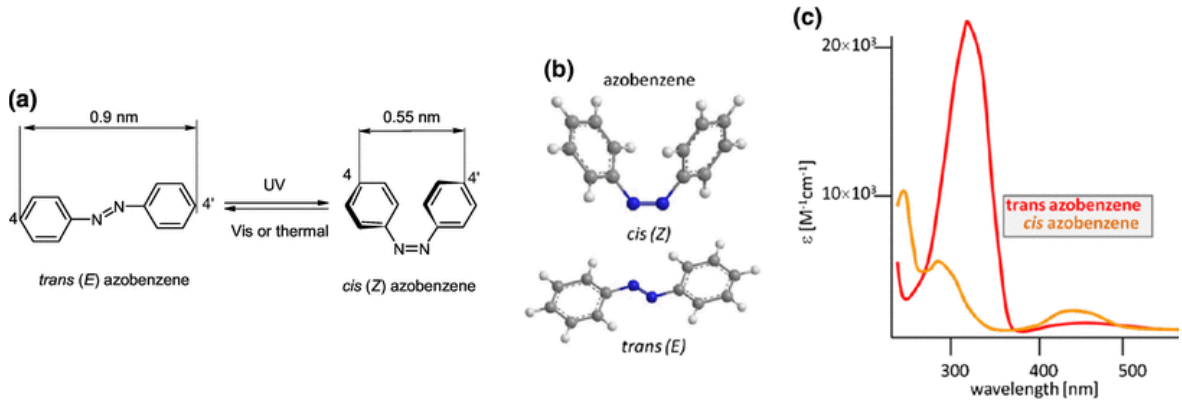

Fig 19: Photoisomerization of Azobenzene (Wagner-Wysiecka, E., Łukasik, N., Biernat, J.F. et al. Azo group(s) in selected macrocyclic compounds. J Incl Phenom Macrocycl Chem 90, 189–257 (2018). https://doi.org/10.1007/s10847-017-0779-4)

CHAPTER 2

Multimerization of small G-protein H-Ras induced by chemical modification at hyper variable region with caged compound

INTRODUCTION

The lipid-anchored small guanine nucleotide binding protein Ras is a central regulator of cellular signal transduction processes leading to transcription, cell cycle progression, growth, migration, cytoskeletal changes, apoptosis, cell survival, and senescence as a molecular switch (1,2). Ras is localized on the plasma membrane through lipid modifications of the hypervariable region (HVR) at the C-terminus (3). Ras assembles into clusters and disassembles on the plasma membrane, and the self-assembly of Ras GTPases significantly affects cell signaling regulation (4). For instance, the dimerization of Ras is essential for Raf-1 activation in the Ras/Raf MEK signal transduction pathway (5). However, the structural basis of homo-multimerization and the fractional distribution of oligomeric states are not well understood.

Many proteins enable physiological functions through the regulation of multimerization. The protein-protein interactions of multimers are based on van der Waals forces, hydrogen bonds, and electrostatic interactions. For example, kinesin forms a dimer or a tetramer via helical interaction, and ATP-driven motor proteins move along and support microtubules and transport various cargos (6,7). The p53 tumor suppressor protein comprises a tetramer via the interaction between helices and is a transcription factor of cellular functions such as cell cycle progression, apoptosis, senescence, and autophagy (8). Thermosomes are hexedecamers, which are archaeal group II chaperonins (9). Ferritin iron storage protein is a 24mer that binds many divalent metals (10). Multimerization may be regulated by external noninvasive stimulation, and the primary method of regulation is stimulation using light. Caged compounds, which are light-sensitive probes, are biologically inert and inactivate the bioactivity of trapped molecules or proteins. These compounds are important tools in the study of various biological phenomena. Light irradiation liberates it and

rapidly recovers its bioactivity selectively and locally (11). Caging small molecules, caged nucleotides, caged EGTA, and caged GABA were used as initiating reagents for bioactivities (12–15). Caged peptides, caged RGD peptides, were used to photoregulate cell adhesion (16). Caged proteins transformed via chemical modification into sensitive residues, notably cysteine and caged zinc-finger nuclease, were used to photoregulate biological activity (17). The 2-nitrobenzyl derivatives are one of the well-known caged compounds applied to biological systems and are hydrophobic molecules that are uncaged after 340–400 nm light irradiation (18–20). In the case of caged peptides, caged C- kemptides were used to photoregulate signal transduction without prior modification or mutagenesis (21). It has also been reported that the bioactivity of caged heavy meromyosin and caged cAMP- dependent protein kinase was recovered by removing the caged group through irradiation (19,22).

In this study, we demonstrated that chemical modification of cysteine residues in HVR using caged chemical compounds instead of physiological lipidation can induce multimerization of Ras. Structural observations using X-ray scattering and electron microscopy suggested that the multimer may reflect the physiological cluster state of Ras as a model in vitro.

MATERIAL and METHODS

Reagents

Ligation enzymes were purchased from Toyobo Co., Ltd. unless stated otherwise. Oligonucleotides were obtained from Sigma Genosys. The apparatus for affinity chromatography on Co2+-NTA agarose was procured from Clontech. Chemicals reagents were purchased from Wako Pure Chemicals unless stated otherwise. The compound 2-nitrobenzyl bromide (NBB) was procured from Sigma-Aldrich.

Expression and Purification of Ras

The cDNA of human H-Ras WT (residues 1–189), plasmids kindly provided by Dr. Sako (RIKEN), was amplified using polymerase chain reaction and ligated into the pET42c vector. We constructed Ras ΔC13 (residues 1–176) plasmids, in which 13 amino acids from the C-terminal were eliminated, and subsequently amplified them by using polymerase chain reaction. The Ras plasmid has three cysteine residues at positions 51, 80, and 118, excluding HVR. We constructed Cys-light Ras plasmids by mutating cysteine 118 to serine. We generated six mutants, C184S/C186S, C181S/C186S, C181S/C184S, C181S, C184S, and C186S with single or double reactive cysteine residues based on the Cys-light Ras plasmid, for further modification with NBB and 4-phenylazomaleinanil (PAM). Ras expression plasmids were used to transform Escherichia coli BL21 (DE3) cells. The Ras was purified using a Co-NTA column. The Co-NTA column was washed with lysis buffer containing 30 mM imidazole, and bound Ras was eluted with lysis buffer containing 100 mM imidazole. The obtained fractions were analyzed using sodium dodecyl sulfate-polyacrylamide gel electrophoresis (SDS-PAGE). Purified Ras was dialyzed with buffer(30 mM Tris-HCl, pH 7.5, 150 mM NaCl, 1 mM MgCl2, and 0.5 mM DTT) and stored at -80 °C until further use.

Modification of cysteine by using NBB

The concentration of the caged compound was varied to suit the type of cysteine. Ras was incubated with 25-times as much NBB as that dissolved in 99.5% ethanol in modification buffer (150 mM NaCl, 30 mM Tris-HCl, pH 7.5, 1 mM MgCl2). DTT was removed using a gel filtration column (10 DG column; Bio-Rad, Hercules, CA, USA) pre-packed with each modification buffer. The cysteine in Ras using NBB was modified by reacting in each modification buffer for 1 h at 25 °C. The reaction was terminated by the addition of DTT to a final concentration of 10 mM and then centrifuged at 15,000 rpm for 15 min at 4 °C. The modified Ras was isolated from the unreacted reagents using a 10 DG column pre-packed with each modification buffer. The stoichiometry of the incorporated NBB in comparison to that of Ras was determined based on the absorption spectrum obtained using an extinction coefficient of 5900 M-1 cm-1 at 350 nm for the NBB group.

Measurement of multimerization by using SEC–HPLC

Size-exclusion chromatography coupled with high-performance liquid chromatography (SEC–HPLC) was performed on a TSKgel G3000PWXL column (TOSOH, Tokyo, Japan; particle size: 6 μm, internal diameter: 7.5 mm, length: 30 cm, injection volume: 20 μl) or a TSKgel SuperSW3000 column (TOSOH, Tokyo, Japan; particle size: 4 μm; internal diameter: 4.6 mm, length: 30 cm; injection volume: 10 μl). Samples (0.5 mg/ml) were eluted with size-exclusion buffers (150 mM NaCl, 30 mM Tris-HCl, pH 7.5, 1 mM MgCl2) at a flow rate of 1.0 or 0.4 mL/min with monitoring of the absorbance at 280 nm, respectively.

Photocontrol of multimerization

Ras was modified with NBB for multimerization as stated in “Modification of cysteine by using NBB” and then photoirradiated at 400 nm (Lambda DG-4, Sutter Instrument Company, CA, USA)

to uncage the 2-nitrobenzyl group on ice. The population ratio of multimers was monitored using SEC-HPLC.

Near- and far-UV CD spectrum measurements

Near-UV CD spectra of a 0.4 mg/ml sample and far-UV CD spectra of a 0.1 mg/ml sample were measured in CD buffer (150 mM NaCl, 30 mM Tris-HCl, pH 7.5, 1 mM MgCl2) at 25 °C using a J- 720 CD spectropolarimeter (JASCO, MD, USA). Ras samples were irradiated at 400 nm for 8 h on ice, and denatured by using 8 M urea. Cuvettes with path lengths of 1 mm and 10 mm were used for the measurements in the near- and far-UV regions, respectively. Each spectrum represents the average of four scans.

Small Angle X-ray Scattering of NBB-Ras

Small-angle X-ray scattering (SAXS) measurements were performed at beam line BL8S3 of the Aichi Synchrotron Radiation Center. NBB-Ras and Ras were measured in SAXS buffer (120 mM NaCl, 30 mM Tris-HCl, pH 7.5, 1 mM MgCl2) at 25 °C with protein concentrations of 2, 4, 6, and 8 mg/ml. The protein solution was inserted into a solution cell with a quartz window. An X-ray beam with a wavelength of 1.5 Å was used. The two-dimensional scattered X-ray pattern was recorded using a Pilatus 100 K detector with square pixels of size 0.172 mm × 0.172 mm placed 2.3 m from the specimen. The exposure time was 180 s for each measurement. A circular average was performed for the two-dimensional SAXS images using FIT2D image processing software (23), in order to obtain one-dimensional intensity profiles as functions of momentum transfer scattering vector length q. The intensity of the scattering profiles was corrected by the incident beam flux measured with the ion chamber placed upstream of the samples. The radius of gyration, Rg(c), and the intensity at zero scattering angle, I(0,c), for each concentration were determined from the Guinier plot of the intensity profile using the PRIMUS program (24) after buffer

subtractions. The Rg(c) and I(0,c)/c data were extrapolated to c = 0 to evaluate the final values at zero protein concentration.

Modeling from X-ray scattering intensity

The conformations of NBB-Ras and Ras were estimated. The distance distribution functions p(r)s were calculated to build structural models from the scattering intensities using the PRIMUS program (24). The dummy-atom models were constructed either without a priori structural information or by assuming a symmetric pentamer structure, and the structural models were obtained by averaging ten structures. These analyses were carried out using the program suite ATSAS (25,26).

Electron Microscopic Observation

The specimens for electron microscopy were prepared according to the method previously reported (27). In brief, NBB-H-Ras or H-Ras were stained with 2% (w/v) uranyl acetate on a carbon- coated grid for 1 min at 23 ◦C, and the solution remained on the grid was removed and dried. The resultant grids were transferred into a transmission electron microscopy (JEM1010; JEOL) operated at 80 kV. Images were recorded on a charge-coupled-device (CCD) camera (FastScan-F214; TVIPS) at a nominal magnification of 20,000 (a pixel size of 6.67 Å).

RESULTS

Chemical Modification of H-Ras with caged chemical compound

We employed a sulfhydryl group-reactive caged compound to modify cysteine residues in HVR. This is because caged compounds can be chemically modified to be introduced into specific amino acid side chains in a protein and then released by using light irradiation to reversibly restore the protein to its original state. NBB was used in this study because it is a well-known cage compound that can be specifically introduced into the thiol group of the cysteine residue, as shown in Fig. 1B (11,20). Then, by light irradiation at 340–400 nm, the nitrobenzyl group was eliminated and the protein reversibly returns to its original state. There are six cysteine residues in H-Ras.

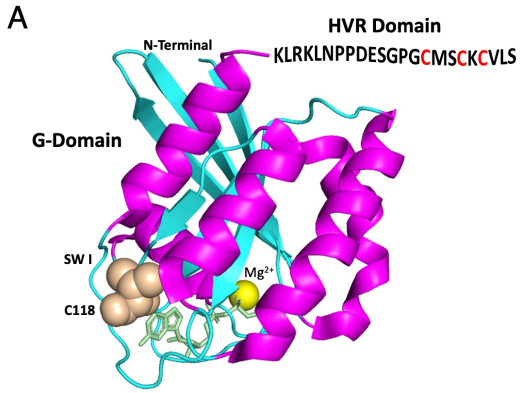

Figure 1. (A) Locations of the cysteine residue in the globular domain and HVR of H-Ras.

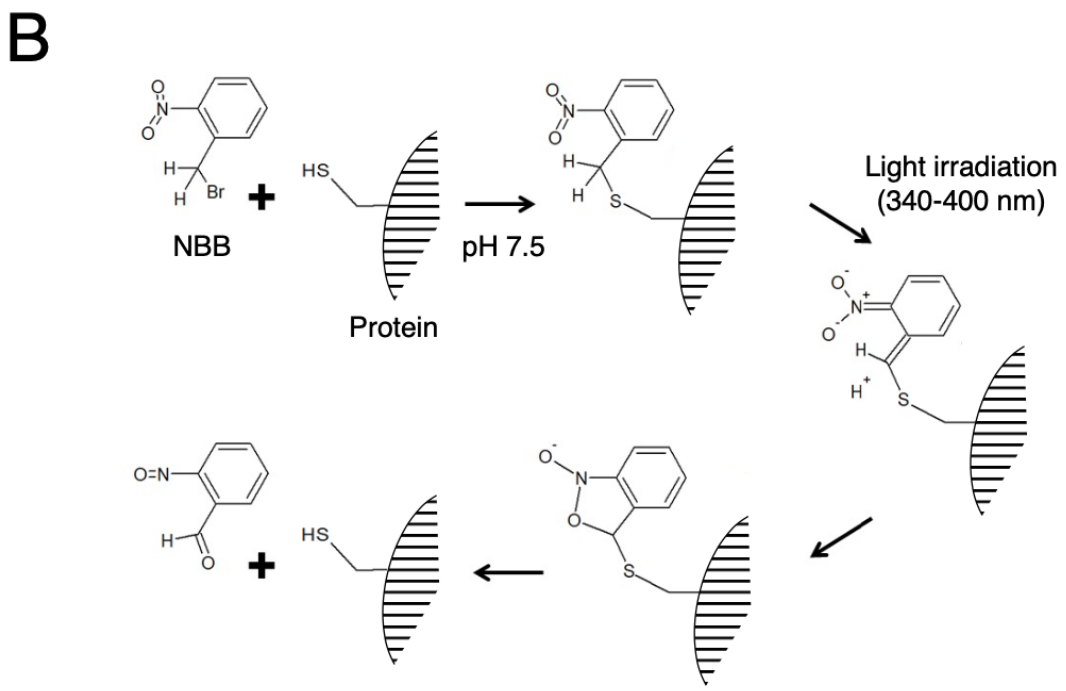

(B) Chemical structure of NBB and the scheme of the chemical modification and uncaging reaction from thiol group of cysteine.

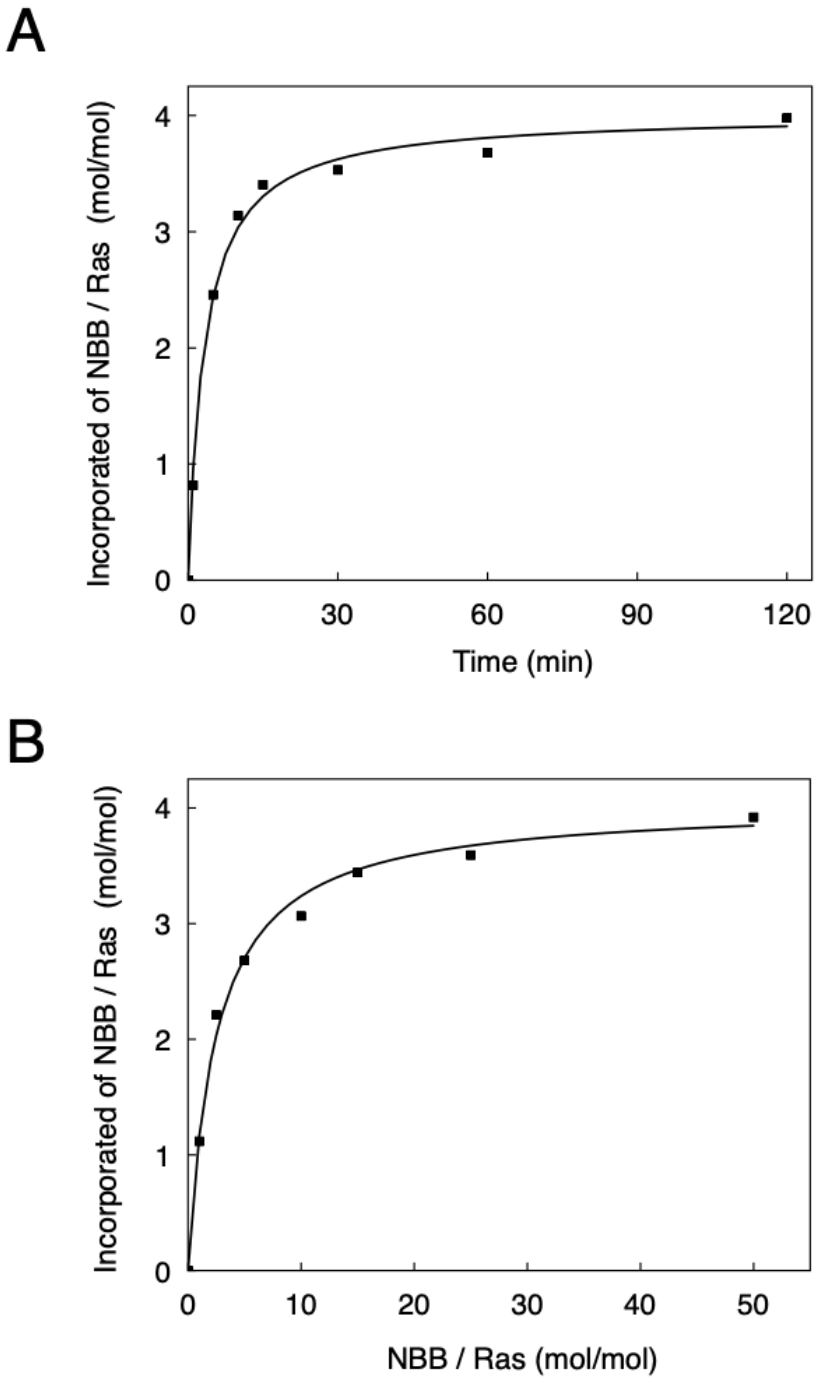

Figure 2. Time-course experiment and the concentration dependence of NBB incorporation into WT H-Ras.

Three of them are in the globular domain, and C118 is located on the surface. The remaining three cysteines (C181, C184, and C186), which are known as lipidation sites, are in the HVR domain. The HVR domain was exposed to the solvent. Therefore, the four cysteine residues were expected to react with the caged compound. Next, NBB was incorporated into cysteine residues stoichiometrically. The time course and concentration dependence of the modification of H-Ras are shown in Fig. 2. The modification was complete within 60 min, and the incorporation of NBB into Ras was saturated at a concentration of approximately 25-fold molar excess of NBB per single molecule of Ras. Four NBB molecules were incorporated into one H-Ras molecule. Therefore, it is assumed that the four cysteine residues (C118, C181, C184, and C186) exposed to the solvent were specifically modified.

Formation of H-Ras multimer induced by chemical modification with caged compound

Multimerization of H-Ras induced by modification with NBB was analyzed using size- exclusion column chromatography. Intact H-Ras eluted at 7.2 ml elution volume as shown in Fig. 3A. A small amount of eluate at 6.8 ml elution volume, which is presumed to be a dimer, was also observed. In contrast, H-Ras modified with NBB was predominantly eluted at 5.4 ml, suggesting the formation of multimers with higher molecular weights. The formation of the multimer significantly depended on the ionic strength (Fig. 3B), indicating that the electrostatic interaction between the units of H-Ras contributed to the higher molecular product. We estimated the apparent molecular weight of the multimer through comparison with the molecular weight standard marker proteins using size- exclusion column chromatography (Fig. 4). In this column, the H-Ras monomer showed an apparent molecular weight of 32 kDa. Conversely, multimers had an apparent molecular weight of 155 kDa. Therefore, it is suggested that H-Ras modified with NBB forms a pentamer.

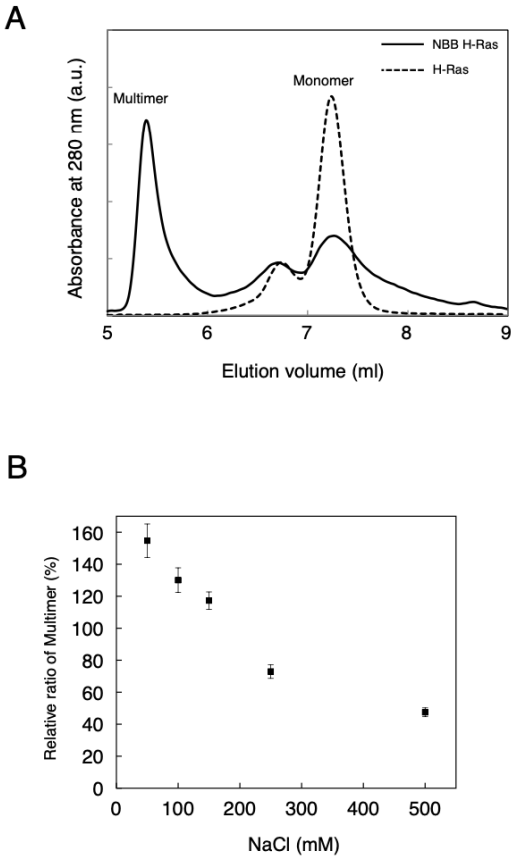

Figure 3. Monitoring the formation H-Ras multimer induced by NBB modification using SEC– HPLC. HPLC. (A) Elution profile of the WT H-Ras modified with NBB. WT H-Ras (10 μM; broken black line) and NBB-WT-H-Ras (20 μM; black line) were injected into SEC-HPLC (TSKgel

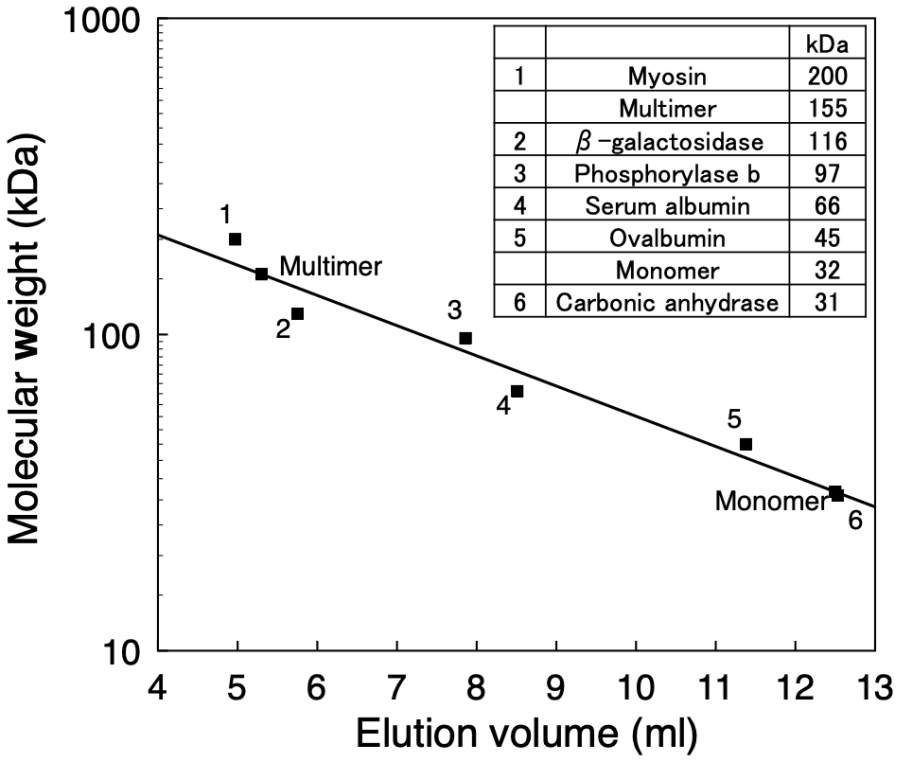

Figure 4 Estimation of relative molecular weight for the NBB-H-Ras multimer from the calibration curve obtained by the retention times of standards on the SEC-HPLC. The retention time of the standard amd the NBB-HRas and intact H-Ras were plotted against the log value of the molecular weight of the standard.

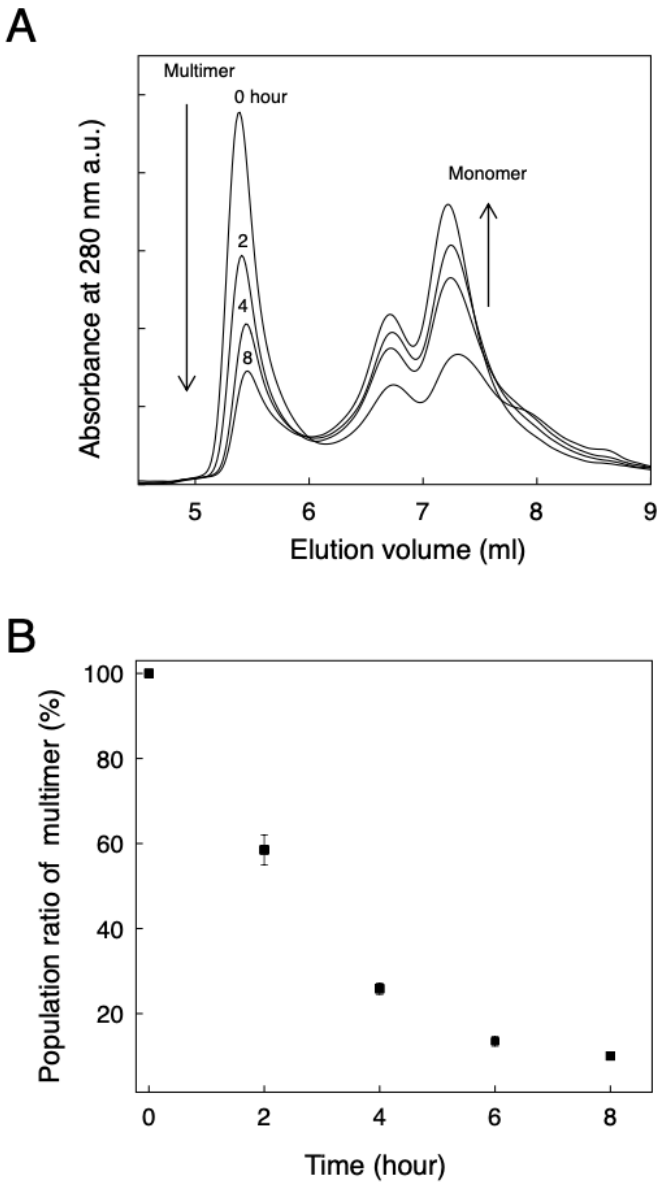

Figure 5 Monitoring the conversion of multimer to monomer by eliminating caged compounds on HVR upon light irrdiation. (A) Light irradiation time dependent changes of elution profile of the NBB-H-Ras on SEC–HPLC. (B) Relative irradiation time dependent decay of the peak coresponding to multimer was esimated from the elution profiles of (A) and plotted agist the irradiation time at 400 nm.

When the caged group was incorporated into H-Ras removed by light irradiation, the Ras multimer was converted to a monomer. As shown in Fig. 5, light irradiation at 400 nm induced a decrease in the peak corresponding to multimer and an increase in the number of monomers in an irradiation time-dependent manner. To confirm that the conversion was not due to denaturation of H- Ras by light irradiation, we measured the CD spectrum of light-irradiated H-Ras. Even after 8 h of light irradiation, no significant changes in the CD spectrum were observed. Therefore, the conversion of a multimer to a monomer is considered to be due to the elimination reaction of the caged group bound to H-Ras by light irradiation.

Identification of the cysteine residue contributing to the formation of H-Ras multimer

To identify which intrinsic cysteine residues are essential for multimerization, we designed eight mutants with cysteine residues substituted by serine or truncated peptides. First, we prepared the mutant C118S, in which cysteine C118 in the globular domain is substituted with serine. NBB was incorporated into the three cysteine residues in the HVR of the C118S mutant (Table I). C118S modified with NBB showed similar efficiency for multimerization (Fig. 8). These results suggest that the modification at C118 is not related to the formation of multimers. Subsequently, we truncated the C-terminal 13 amino acid residues, including the three cysteine residues, C181, C184, and C186, in the HVR. The truncated H-Ras mutant ΔC13 did not form a multimer by NBB modification at C118. Therefore, it is clear that cysteine residues in the HVR are required to form multimers. Furthermore, mutants in which one or two of the cysteine restudies in the HVR were replaced by serine residues were also prepared. The number of NBBs incorporated into each mutant is summarized in Table I. The expected incorporation of NBB into the remaining cysteine residues of each mutant. As shown in Fig. 8, the mutants C181S, C184S, and C185S, in which one of the cysteines in HVR is substituted by other amino acids, showed a 30% reduction in multimer

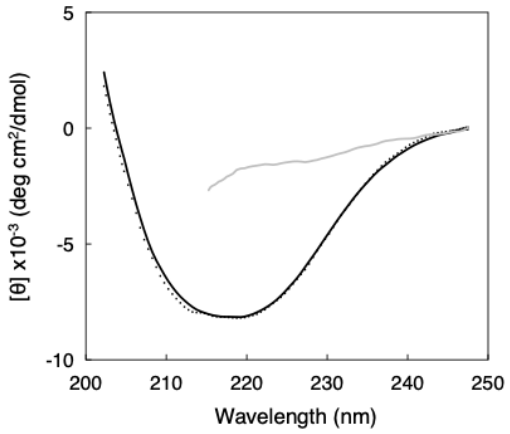

Figure 6 Far-UV CD spectrum of NBB-Ras irradiated by light. Far-UV CD spectra of 0.1 mg/ml NBB-Ras was measured before (solid line) and after (dotted line) light irradiation at 400 nm. Light irradiation at 400 nm was performed for 8 h at 0 °C. The thin gray line indicates NBB-Ras denatured in the presence of 8 M Urea.

Table I. Incorporation efficiency of caged compound into Ras

	NBB/Ras. (mol/mol)
WT	4.12 ± 0.15
ΔC13	1.12 ± 0.04
C118S	3.28 ± 0.08
C118S/C184S/C186S	1.26 ± 0.04
C118S/C181S/C186S	1.11 ± 0.05
C118S/C181S/C184S	1.22 ± 0.04
C118S/C181S	2.09 ± 0.03
C118S/C184S	2.15 ± 0.12
C118S/C186S	2.03 ± 0.06

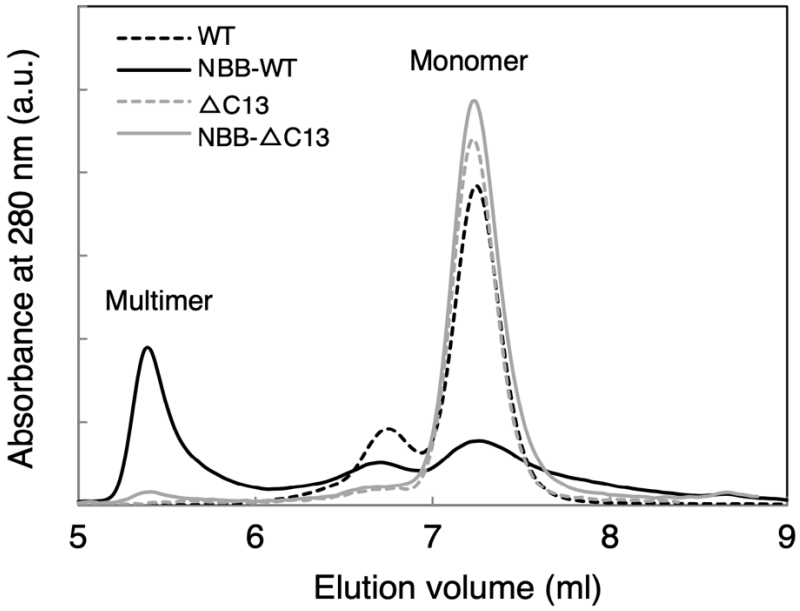

Figure 7 Elution profile of the H-Ras (ΔC13 H-Ras) modified with NBB in which 13 C-terminal amino acid residues, including three cysteine residues, were truncated. Samples of WT (10 μM; broken black line), NBB-WT (black line), ΔC13 (broken gray line), and NBB-ΔC13 (gray line) were injected into SEC-HPLC equilibrated with 150 mM NaCl, 30 mM Tris-HCl, pH 7.5, 1 mM MgCl2.

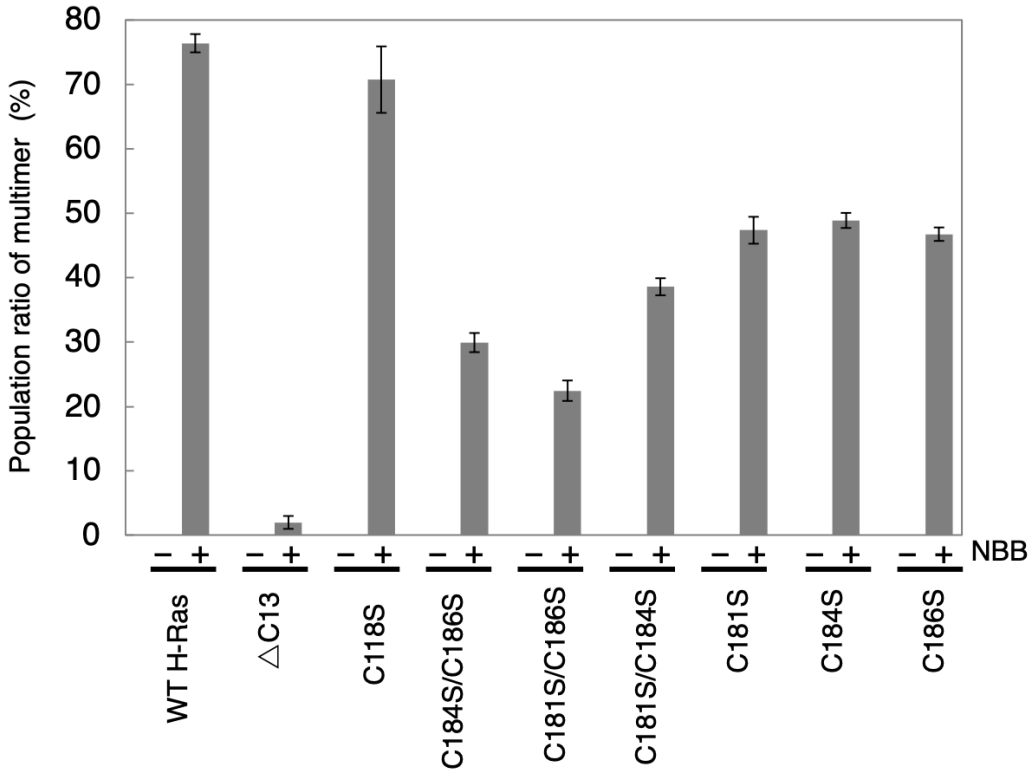

Figure 8 Population rate of the multimers formed by NBB modification for the H-Ras mutants in which cysteine residues were substituted by serine residue. Ras mutants modified with NBB were injected into SEC-HPLC and the population of the multimer were estimated from the elution profiles.

formation. The mutants C181S/C184S, C184S/C186S, and C181S/C186S, in which a single cysteine residue was retained in HVR, decreased the ratio of multimer formation by 50%, 40%, and 30%, respectively. The results suggest that the formation of multimers depends on the number of NBBs incorporated into the HVR. All three cysteine residues in HVR are essential for the efficient formation of Ras multimer by modification with NBB.

Structural analysis of NBB-Ras multimer by X-ray small-angle solution scattering and dummy-atom structural modeling

To study the global conformation of the multimer of H-Ras induced by NBB modification at HVR, we utilized a small-angle synchrotron X-ray scattering technique using synchrotron radiation. H-Ras (2, 4, 6, and 8 mg/ml) modified with NBB in a buffer containing 120 mM NaCl, 30 mM Tris-HCl, pH 7.5, and 1 mM MgCl2 were measured at 25 °C. Intact Ras and NBB-H-Ras irradiated with 400 nm wavelength light for 2h (ΔNBB-H-Ras) were also measured for comparison. The radius of gyration, Rg(c), and the intensity at zero scattering angle, I(0,c), for each concentration were determined from the Guinier plot of the intensity profile. The concentration dependence of the Rg(c) and I(0,c) values was linearly approximated.

As shown in Fig. 9A, the plot of I(0)/c vs. c clearly indicates that the estimated molecular weight of NBB-H-Ras is five times larger than that of intact H-Ras. Therefore, the multimer composed of NBB-H-Ras was revealed to be a pentamer, which is consistent with the results of size exclusion chromatography (Fig. 4). ΔNBB-H-Ras, in which the 40 % NBB group was eliminated by light irradiation, showed much reduced molecular weight, suggesting the conversion of pentamer to monomer. Possible dummy-atom structural models of the NBB-H-Ras were estimated from the data analysis of scattering intensities according to the method described in the Materials and Methods section. Two possible structures were obtained, as shown in Fig. 10. One was assumed to have a five-fold symmetry (Fig. 10A). Notably, the symmetric pentamer model of the NBB-H-Ras multimer was similar to one of the models estimated for the cluster of K-Ras by an in silico study reported by Sarkar-Banerjee et al (28). The other model also shows a ring structure, which results from the calculation with no symmetric assumption (Fig. 10B).

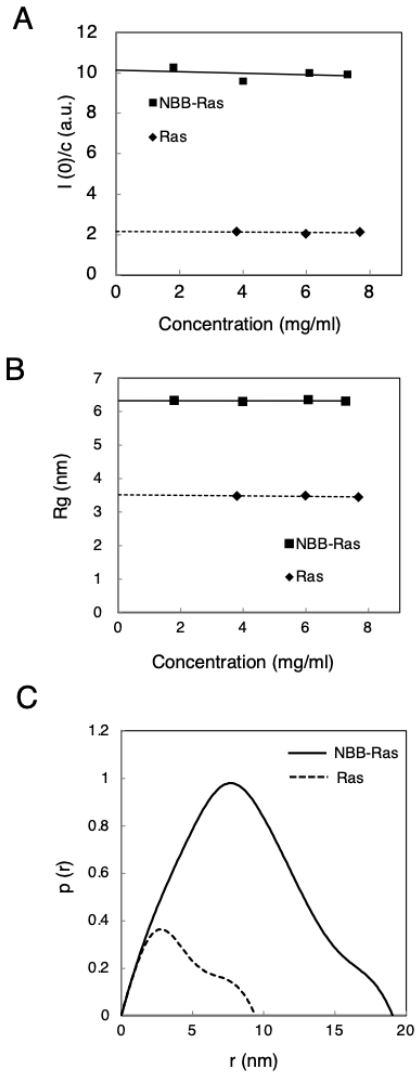

Figure 9 Small angle solution X-ray scattering analysis of Ras multimer. (A) The protein concentration dependence of [I(0)/c] evaluated from Guinier plots. Solid and dashed lines represent linear approximations. Relative molecular weights can be obtained from the intercept. (B) The protein concentration dependence of the radii of gyration (Rg). (C) The p(r) functions of NBB-Ras and control H-Ras calculated from scattering intensities.

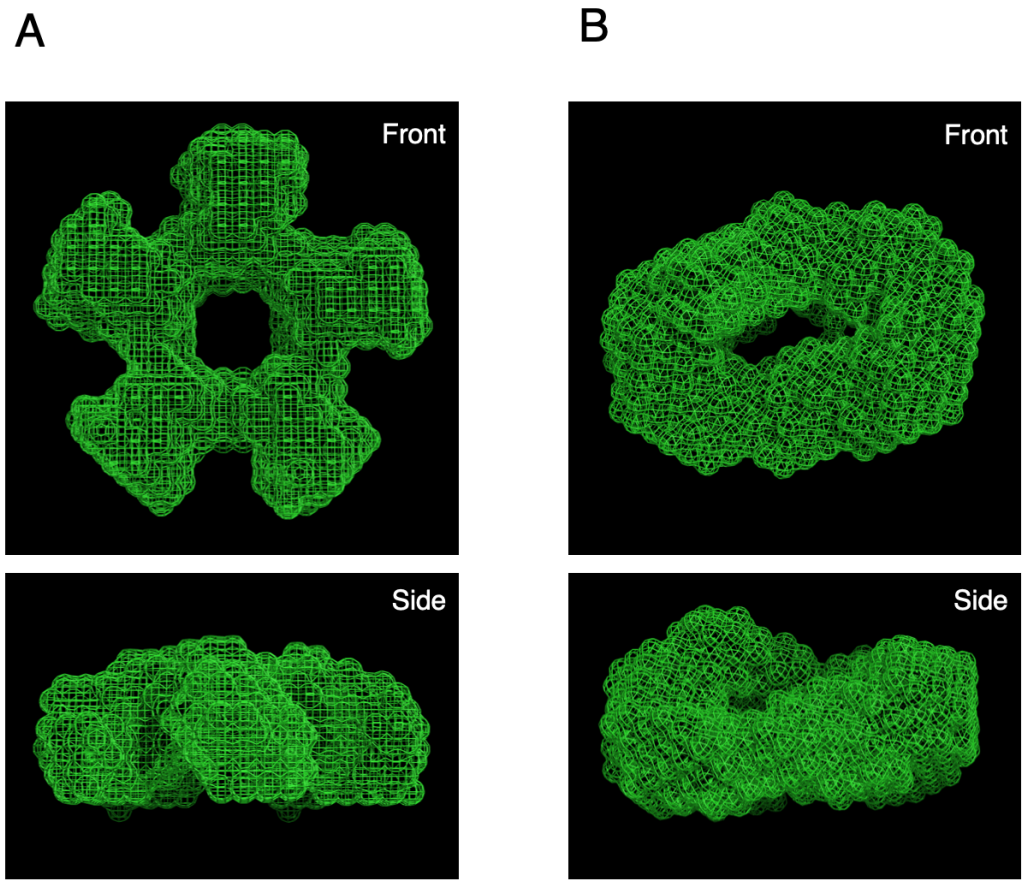

Figure 10 Possible structures estimated from small angle X-ray scattering. Possible structures for NBB-Ras estimated from small-angle X-ray scattering. The dummy-atom structural models were obtained using the DAMMIF program. (A) The model was assumed to have five-fold symmetry. (B) The model was calculated similar to that in (A) but without the assumption of any symmetry.

Electron microscopic observation of the Ras multimer

Using negative staining and transmission electron microscopy, we observed the configurations of the NBB-H-Ras multimer and intact H-Ras monomer. As shown in Fig. 11A, H-Ras modified with NBB showed apparently round-shaped particles with a diameter of approximately 20 nm, which is consistent with the size of the multimer estimated from P(r) function X-ray scattering. Conversely, such a particle reflecting the formation of multimers was not observed. Only indistinguishable small particles, which may correspond to the monomer of H-Ras, were observed (Fig. 11B). Electron microscopic observation of NBB-H-Ras strongly suggested the formation of a multimer with a round shape. After averaging and overlapping 500000 of molecules using EMAN2 software a donut shape structure was found which shown in Fig. 11C.

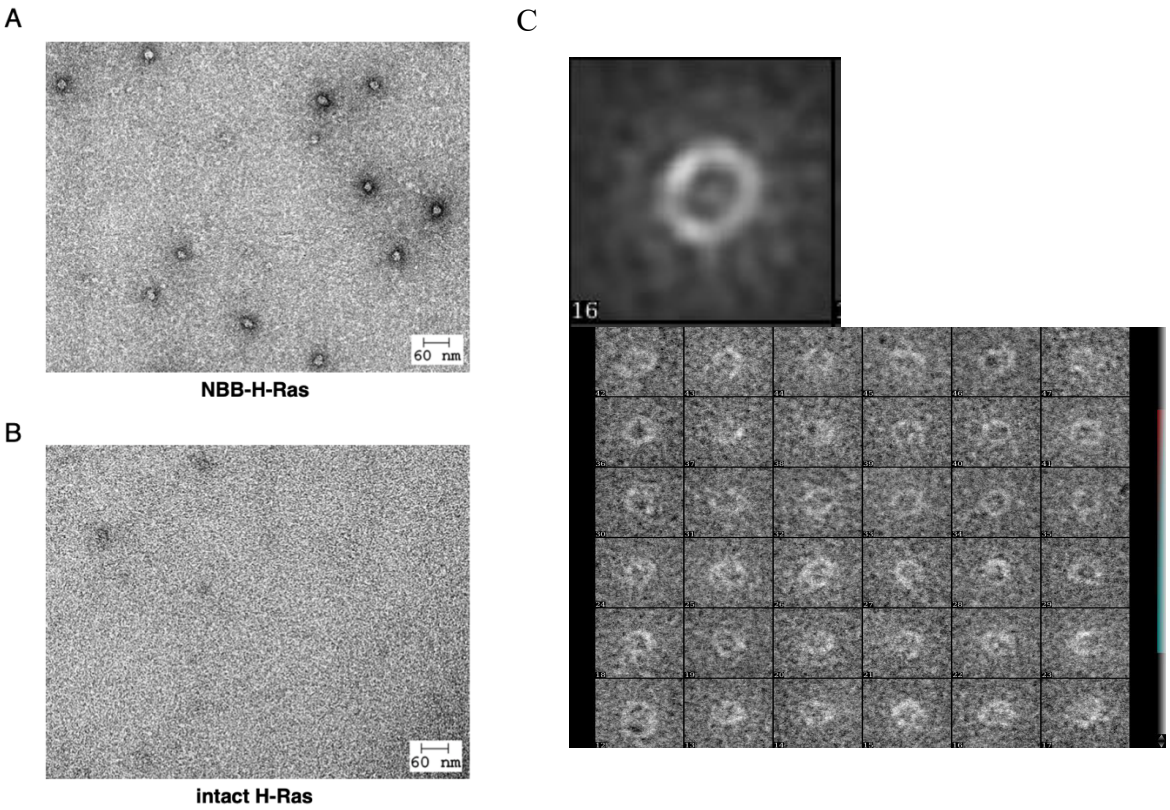

Figure 11 Electron microscopic observation of Ras multimer. Negative staining images of the H-Ras modified with NBB (A) and intact H-Ras (B) obtained using transmission electron microscopy.

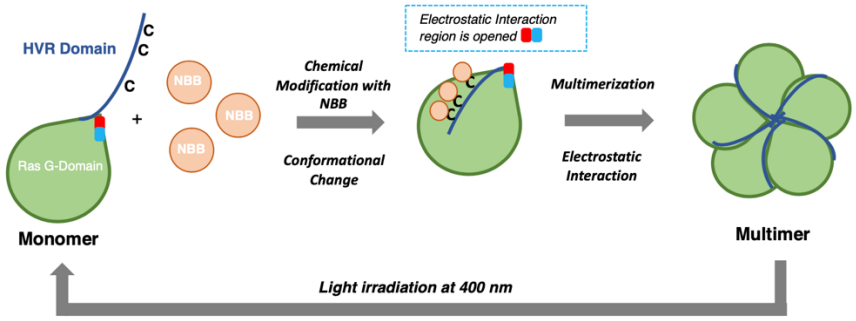

Figure 12 Proposed possible mechanism for multimerization of H-Ras with NBB.

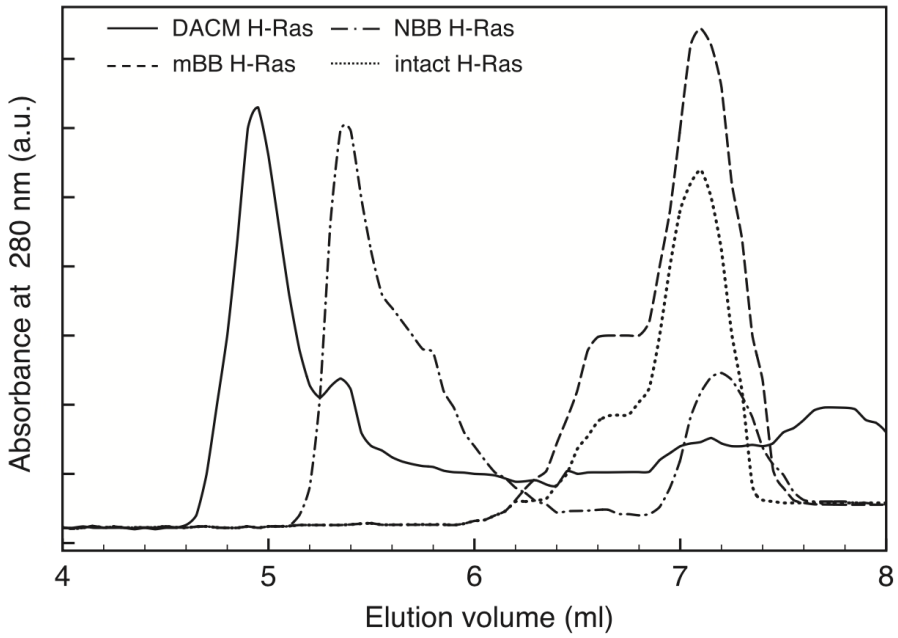

Fig. 13. Elution profile of the WT H-Ras modified with DACM and mBB on SEC-HPLC. WT H-Ras (), NBB-WT-H-Ras (), DACM-WT-H-Ras () and mBB-WT-H-Ras () were injected into SEC-HPLC (TSKgel G3000PW$_{XL}$ column) equilibrated with 150-mM NaCl, 30-mM Tris–HCl, pH 7.5 and 1-mM $MgCl_2$.

DISCUSSION

Physiological studies have revealed that plasma membrane- bound Ras forms transient nanoclusters of oligomers and regulates effectors (28). Therefore, multimerization is essential for the transmission of cell signals. Lipidation of cysteine residues in HVR induces the localization of Ras to the plasma membrane and the formation of multimers. However, the structural basis of multimers related to physiological function has not been clarified because physiological conditions are difficult to examine. In this study, we demonstrated that chemical modification of cysteine residues in HVR by a caged compound, NBB, instead of physiological lipidation, induces the formation of a stable multimer of H-Ras. The removal of caged compounds by light irradiation converts multimers into monomers. Notably, our proposed pentamer model of the NBB-H-Ras multimer estimated from the x-ray scattering analysis (Fig. 10) and electron microscopic observation (Fig. 11) showed high similarity with one of the structural models of a pentameric K-Ras nanocluster observed in an in silico study (27). A unique symmetrical pentagonal ring shape was observed among the structures estimated from these analyses. The artificial multimer induced by chemical modification may mimic the physiological nanocluster of Ras in vitro.

We examined various cysteine-reactive reagents to form multimers. Some of the compounds induced multimers in a manner similar to that of NBB. For instance, the thiol reactive fluorescent probe, N-(7-dimethylamino-4- methylcumarin-3yl) maleimide, also induced the formation of multimers of Ras with a slightly higher molecular weight than that of NBB modification, as shown in Fig. 13. This suggests that physiological transient nanoclusters of various sizes (29) can be formed by modifying the reagents. However, these compounds cannot be reversibly incorporated or eliminated by external stimuli. The caged compound used in this study has the advantage of

being able to reversibly induce multimerization and monomerization of H-Ras by chemical modification and photoelimination reactions. This is expected to be applied to the optical control of G-proteins. In contrast, some thiol-reactive fluorescent compounds, such as bis (2,5,6-trimethylpyrazolo [1,2-a] pyrazole-1,7-dione-3-ylmethyl) sulphide and monobromobimane did not induce multimer formation (Fig. 13). Therefore, a specific structure of the compound to be modified is required for the formation of H-Ras multimers. This suggests that it is possible to control the formation of multimers and monomers photoreversibly by introducing a photochromic compound whose structure and properties change drastically. As a preliminary experimental result, we have shown that the efficiency of multimer formation was partially altered by cis-trans photoisomerization by an azobenzene derivative incorporated into cysteine of HVR (unpublished data). The driving force for multimer formation may be primarily dependent on intermolecular electrostatic interactions. As the con- centration of NaCl increased, the formation of multimers was significantly reduced (Fig. 3B). Currently, the amino acid residues involved in the direct intermolecular inter- actions among the subunits in the Ras multimer induced by NBB modification have not been identified. Therefore, analysis at the molecular level, such as high-resolution cryo-electron microscopy, is required to show the amino acid interactions in further studies. Possible regions con- tributing to the intermolecular association among NBB- H-Ras can be presumed from the study of the K-Ras mutant. Sarkar-Banerjee et al. (27) reported that K-Ras mutants K101E and K101C/E107C destabilize and stabilize multimers, respectively. Hence, these amino acid residues may be involved in direct interactions intermolecularly or indirectly to form multimers. Some related studies have reported the indirect interaction of these amino acid residues. It has also been shown that loop 7 (107– 110) containing E107 communicates with the catalytic site allosterically (30, 31). K101 is in helix 3 and is located near E107. The distance between the

two amino acid residues is close enough to form a salt bridge intramolecularly on the crystallographic observation of K-Ras. Helix 3 contains K104, which is known as a site of acetylation and ubiquitination (32, 33). Therefore, helix 3 has an important region related to the physiological function of Ras. The salt bridge between K101 and E107 may stabilize the relative spatial conformation around the regions of helix 3 and loop 7. The stabilized conformation may be essential for multimer formation. For H-Ras, the basic and acidic amino acids of K-Ras were conserved as K101 and D107, respectively. Notably, the amino acid residues in the globular domain were located near the base of the tail-shaped HVR. For H-Ras, incorporation of NBB into HVR may induce a conformational change of HVR to interact with helix 3 and loop 7 regions to form intermolecular electrostatic interactions allosterically, resulting in multimer formation. To support this speculation, it has been reported that the relative conformation of the HVR and G-domain changes dramatically when Ras interacts with the cell membrane to transmit cell information (31,32).

CONCLUSION

In conclusion, we demonstrated that the chemical modification of H-Ras with caged compounds at the lipidation site in the domain of HVR-induced multimerization of H-Ras, which may reflect the physiologically transient functional state of the H-Ras cluster. It is expected that the modification of HVR with an external stimulus response can be applied to the structural analysis of physiologically functioning Ras multimers at the molecular level and control artificial cell signal transduction.

CHAPTER 3

Photocontrol of GTPase cycle and multimerization of the small G-protein H-Ras using photochromic azobenzene derivatives

INTRODUCTION

The small GTPase Ras acts as a binary switch in the signal transduction pathways to control cell growth, differentiation and proliferation by cycling between the off state of GDP bound and switch on state of GTP bound states (1, 2). Two factors regulate the active ON state and inactive OFF state of Ras. GTPase activating protein (GAP) induces hydrolysis of GTP to GDP, resulting in the formation of an inactive state of Ras. On the other hand, the guanine nucleotide exchange factor (GEF) replaces GDP with GTP and makes the Ras ON state. Switching mechanisms utilizing conformational changes in nucleotide-binding motifs have been well studied at the molecular level (3). Interestingly, recent structural studies indicated that G proteins contain a conserved nucleotide binding motif with ATP driven motors, kinesin and myosin. These nucleotide-binding proteins might have evolved from a common nucleotide binding ancestral protein and share a common catalytic core region, including P-loop, Switch I and Switch II, and molecular mechanisms utilizing a nucleotide hydrolysis cycle (4). Previously, we demonstrated that incorporating artificial regulatory nanodevices, such as photochromic molecules, into the kinesin functional site enables the photoreversible regulation of ATPase activity (5, 6, 7). Subsequently, we incorporated azobenzene derivatives into the functional sites of the motor domain and succeeded in photocontrolling GTPase activity (8). H-Ras has a specific unique functional domain of the hypervariable region (HVR) located at the C-terminus that plays a physiologically important role. It is known that cysteine residues in HVR are modified by farnesylation and palmitoylation. Lipidation enables H-Ras to bind to the membrane and form clusters, resulting in intracellular signal transduction. It is known that the location of lipidated HVR in the globular domain is different from that of unlipidated H-Ras (9, 10). Therefore, the conformational change in HVR

determines the physiological performance of Ras. We have recently demonstrated that chemical modification of the cysteine residues in the HVR of Ras with SH group reactive caged compounds instead of lipidation induces multimerization of Ras, which may mimic the physical cluster structure (11). The multimer returned to the monomer by eliminating the caged group from the HVR by light irradiation. The results suggested that incorporating a specific group into the lipidation site of HVR may induce artificial physiological structural changes related to Ras function. However, the caged compound exhibits an irreversible photoelimination reaction (12). Therefore, the caged components do not work as a reversible photo-switch. In the present study, we utilized an azobenzene derivative as a photo-reversible nano-switching device and incorporated it into the HVR to control the Ras function.

MATERIALS AND METHODS

The Toyobo (Tokyo) products of restriction enzymes and related enzymes from were used. The designed cDNA was synthesized using Integrated DNA Technologies (Japan). Affinity chromatography on Co^{2+}-NTA agarose Clontech (CA, USA) was used to purify the recombinant Ras and related proteins. PAM was purchased from Sigma-Aldrich (MO, USA). BIOMOL GREEN was purchased from Enzo (Tokyo, Japan).

Expression and Purification of Ras mutant

The cDNA of human H-Ras WT (1-189) plasmids offered by Dr. Sako (RIKEN), was amplified by PCR and incorporated into the pET42c vector with the general ligation procedure. We constructed the plasmid of the mutant H-Ras in which cysteine 118 substituted by serine (C118S) to delete reactive cysteine residue in the globular domain of Ras. Ras expression plasmids were transformed into *Escherichia coli* Rosetta2 (pLysE; Invitrogen, CA, USA). The Ras was purified according to the established methods with a Co^{2+}-NTA column. Purified Ras in the stock solution buffer, 150 mM NaCl, 1 mM $MgCl_2$, 30 mM Tris-HCl (pH 7.5), and 0.5 mM DTT was stored in the deep freezer.

Expression and Purification of GEF and NF1

The cDNA GEF and NF1 (GAP GRD domain) were designed with a multi-cloning site (MCS) for three different vectors. The two vectors, pET-21a and pET-15b, were chosen based on their availability in the laboratory. The designed cDNA was then synthesized by Integrated DNA Technologies (IDT, Japan). The synthesized cDNA of NF1 and SOS with a multi-cloning site was treated with the chosen restriction enzymes and ligated into the pET-21a and pET-15b vectors, respectively. NF1 and GEF expression plasmids were transformed into *Escherichia coli* Rosetta2 (DE3) pLysS (Invitrogen, CA, USA). GEF and NF1 were purified with Co^{2+}-NTA columns.

Purified NF1 in the buffer of 150 mM NaCl, 1 mM $MgCl_2$, 30 mM Tris-HCl (pH 7.5) and 0.5 mM DTT was stored in the deep freezer (-80 ℃. Purified GEF in the buffer of 150 mM NaCl, 1 mM $MgCl_2$, 30 mM Tris-HCl (pH 7.5), 0.5 mM DTT, and 0.1% CHAPS was stored in the deep freezer (-80 ℃) until further use.

Synthesis of CASAB

The synthesis of 4-chloroacetoamido-4′-sulfo-azobenzene (CASAB) was performed in a single-step reaction between 4-aminoazobenzene-4′-sulfonic acid sodium salt (167.06 μmol) and chloroacetic anhydride (417.65 μmol). The ratio of the reaction was 1:2.5, and reacted for 30 min in 1 ml dry N, N-dimethylformamide (DMF) at 25 °C and stirred with a magnetic stirrer. The expected product was purified with a large TLC (PLC silica gel60, MERCK) with 20% methanol and 80% chloroform as a developing solvent. CASAB showed Rf value 0.26. The synthesis of the compound CASAB was confirmed by fast atom bombardment mass spectrum. The products showed a molecular ion at m/z 352+1 corresponding to a molecular mass of 353.781 of CASA formula.

Photoirradiation for isomerization of Ras modified with PAM and CASAB

The isomerization of PAM and CASAB was performed at 0 °C using UV-light irradiation generated with Black-Ray lamp (16 W) (UVP Inc., San Gabriel, USA) at 366 nm for induction of the *cis* state and by VIS light irradiation using a room fluorescent lamp (27 W) to induce the *trans* state.

Modification of H-Ras HVR domain using PAM and CASAB

PAM: The modification of the HVR domain with PAM was performed as following procedure. H-Ras (5 μM) reacted with PAM (18 μM) in the reaction buffer (120 mM NaCl, 30 mM Tris-HCl pH 7.5) with 3% DMF at 25 °C for 10 min. The reaction was stopped by addition of DTT to a final

concentration of 2 mM. Subsequently the unreacted reagents was removed using a gel filtration column (10 DG; Bio-Rad, Hercules, CA, USA) pre-packed with the buffer of 30 mM Tris-HCl (pH 7.5), 120 mM NaCl. The stoichiometric incorporation of PAM was estimated using an extinction coefficient of PAM (10,620 M^{-1} cm^{-1} at 350 nm).

CASAB: The modification of the HVR domain using CASAB was carried out by reacting H-Ras (5 μM) and CASAB (40 μM) in the reaction buffer (120 mM NaCl, 30 mM Tris-HCl pH 8.0) with 3% DMF for 12 h at 25 °C in the dark. The reaction was stopped by addition of DTT to a final concentration of 2 mM. The modified H-Ras was separated from the unreacted reagents using a gel filtration column (10 DG; Bio-Rad, Hercules, CA, USA) equilibrate with the buffer 30 mM Tris-HCl pH 8.0 and 120 mM NaCl. The stoichiometric incorporation of CASAB was estimated according to the same method used for PAM.

Measurement of the GTPase activity

GTPase activity was determined using a previously established method. H-Ras (2 μM) in GTPase activity assay buffer 30 mM Tris-HCl pH 7.5, 60 mM NaCl, 2 mM $MgCl_2$ was pre-incubated for 5 min in the presence of 2 μM GAP and GEF. Subsequently, 1 mM GTP was added to initiate GTPase assay at 25 °C for 30 min and stopped by addition of 10 % trichloroacetic acid (TCA). After centrifugation for 5 min at 15000 rpm at 4 °C, the supernatant was mixed with BioMol Green Reagent and incubated at 25 °C for 30 min to determine the amount of Pi generated by GTP hydrolysis quantitatively.

Cis isomer of Ras modified with PAM or CASAB was induced by UV light irradiation (Black-ray lamp, 366 nm, 16 W, UVP Inc., San Gabriel, CA, USA) for 3 min. And Ras modified with PAM or CASAB was irradiated by visible light (Fluorescent lamp 27 W, FML27EX-N, Mitsubishi Inc.,

JP) to convert to *trans* isomer for 10 min. The GTPase activity of Ras modified with PAM or CASAB was measured at 25 °C in a GTPase assay buffer.

Size-exclusion Column Chromatography Coupled with High-performance Liquid Chromatography

Size-exclusion column chromatography coupled with high-performance liquid chromatography (SEC–HPLC) was performed on a TSKgel G3000PW$_{XL}$ column (TOSOH, Tokyo, Japan, φ7.5 mm x 30 cm) or a TSKgel SuperSW3000 column (TOSOH, Tokyo, Japan, v4.6 mm x 30 cm). 0.5 mg/ml samples were eluted with size-exclusion buffer, 30 mM Tris-HCl pH 7.5, 120 mM NaCl at a flow rate of 1.0 or 0.4 ml/min with monitoring of the absorbance at 280 nm.

RESULTS

Modification of cysteine residues in HVR with azobenzene derivatives

We utilized the two thiol group-reactive azobenzene derivatives N-(4-phenylazophenyl) maleimide (PAM) and 4-chloroacetoamido-4′-sulfo-azobenzene (CASAB) to incorporate cysteine residues as lipidation sites in HVR in order to photocontrol the H-Ras function. As shown in Figure 1, PAM and CASAB exhibit *cis* and *trans* isomerization by UV and visible light irradiation, respectively. Their isomerization induces alterations in significant molecular size and polarity. PAM is relatively hydrophobic and is expected to have a similar effect to lipidation. On the other hand, CASAB contains a highly negatively charged sulfo group. Therefore, CASAB is expected to exhibit different effects on the Ras function from PAM. To show the optimal conditions to label the cysteine residues in HVR with the azobenzene derivatives, time course and concentration dependence reactions were examined. In this study, we prepared an H-Ras mutant, C118S, in which the C118cysteine residue on the globular domain surface was replaced by serine. Therefore, the H-Ras mutant contains three reactive cysteine residues in HVR. The incorporation of PAM into H-Ras was very quickly saturated with modification time >1 min (data not shown). This is consistent with our previous experimental data of the fast modification of kinesin and calmodulin with PAM (13, 5). The PAM concentration-dependent experiment indicated that the modification of Ras with PAM was saturated at approximately four times the amount of Ras, as shown in Figure 3A. At the initial saturated concentration of approximately 20 μM, The three cysteine residues in the HVR of H-Ras mutants were almost stoichiometrically modified by PAM (Cys residues in HVR:PAM = 3.0 : 3.2). On the other hand, CASAB showed a quite different reaction profile from PAM. The reaction of CASAB with H-Ras C118S was very slow. It took more than 10 h to saturate the HVR. Interestingly, the incorporation of CASAB into C118S showed saturation at the ratio of

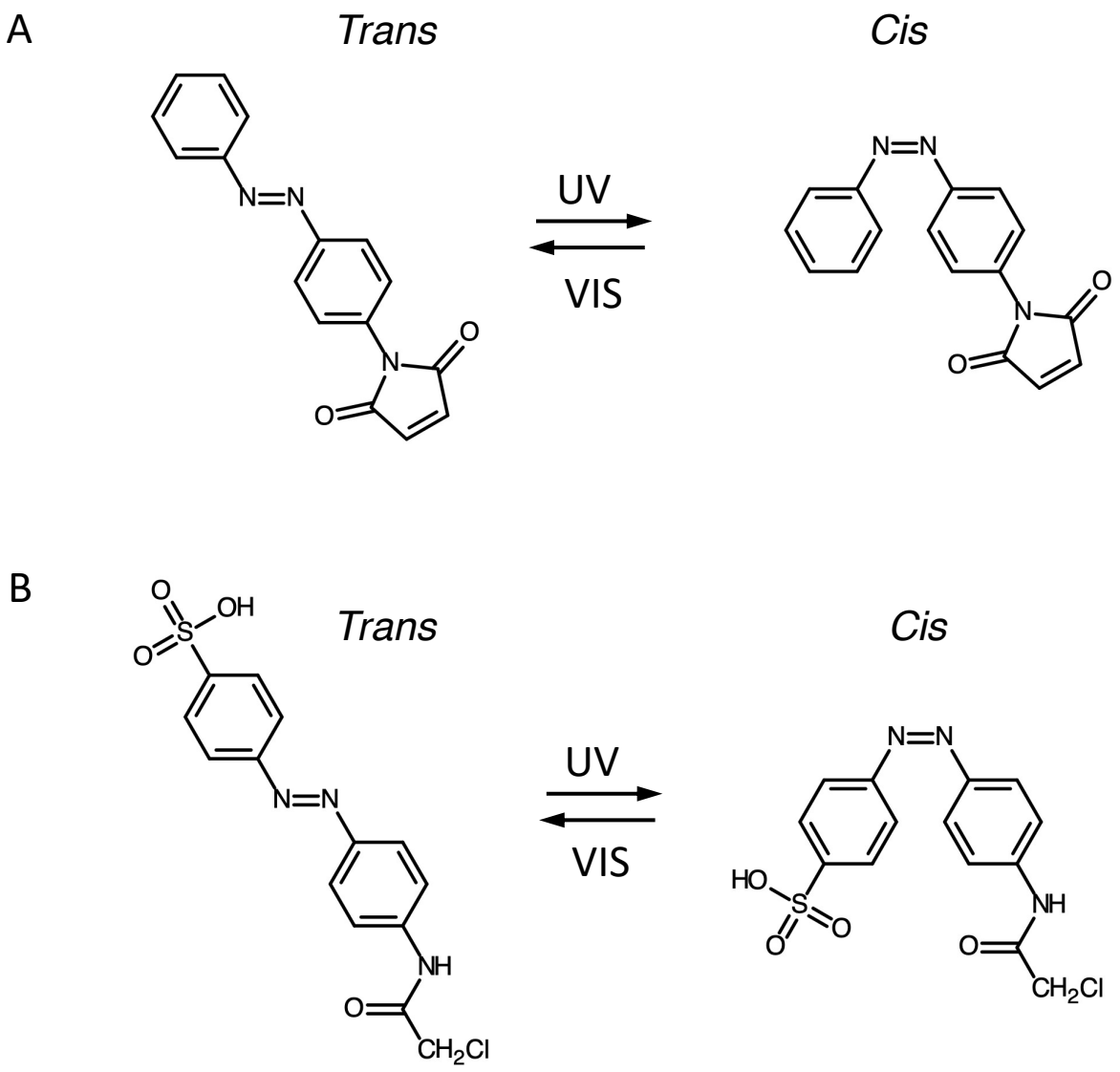

Figure 1. Chemical structure and photo-isomerization of the azobenzene derivatives, (A) PAM and (B) CASAB.

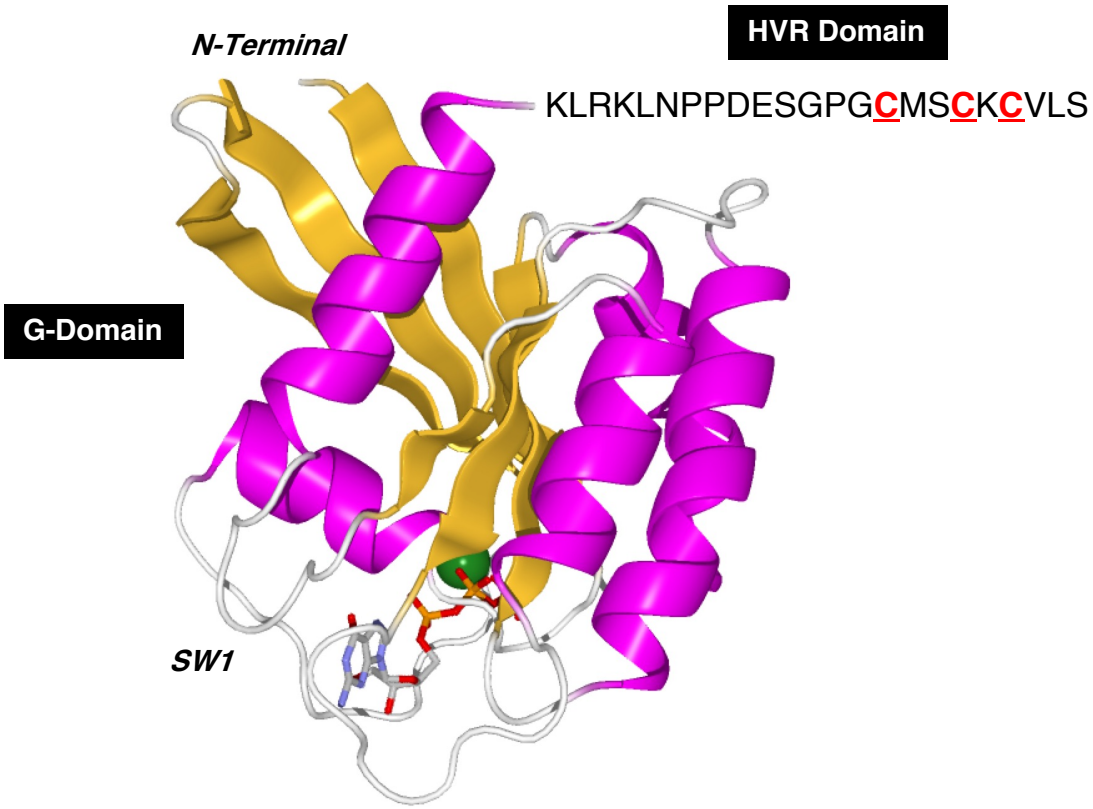

Figure 2. Locations of the cysteine residue in the globular domain and HVR of H-Ras. C181, C184, and C186 in HVR are shown in red. The three-dimentional structure was drawn using Mol Feat 4.0 (the molecular graphics program) using the data of PDB(1QRA) of H-Ras. GTP and Mg^{2+} are shown in stick and ball, respectively.

Cys residues in HVR:CASAB = 3 : 2. These results suggest that two of the cysteine residues among the three cysteine residues in HVR were specifically modified. As shown in Figure 2, the cysteine residues in the HVR were located very close to each other. Therefore, a possible explanation for the insufficient stoichiometric incorporation is the strong intermolecular negative charge repulsion between the sulfonate groups in the CASAB molecules.

Photoisomerization of azobenzene derivatives incorporated into HVR of H-Ras

We can monitor the isomerization states, *cis* or *trans* of azobenzene and its derivatives by measuring UV/VIS light absorption spectroscopy (14). The absorption spectra of CASAB and PAM showed almost identical spectra and exhibited significant spectral changes upon UV and visible light irradiation, reflecting typical azobenzene *cis* and *trans* isomerization (Figures 4A, B and 5A, B). The *trans* state of free PAM showed maximum absorption at 340 nm, and the peak was significantly reduced by UV irradiation. The change of the spectrum was very fast and completed within 2 min. On the other hand, although PAM-modified H-Ras showed a similar absorption spectrum, the peak of the spectrum exhibited a slower reduction than free PAM with 10 min UV irradiation to be saturated. Visible light irradiation induced absorption recovery at 340 nm for free PAM, as shown in Figure 4C, reflecting *cis* to *trans* isomerization. The *cis* to *trans* isomerization under this condition was slower than the isomerization of *trans* to *cis* upon UV irradiation. It took at least 10 min to obtain a saturated spectrum by Visible light irradiation. Free CASAB-and CASAB-modified H-Ras showed almost similar spectral changes to free PAM and PAM-modified H-Ras, respectively, as shown in Figure 5. The results suggested that the azobenzene derivatives incorporated into H-Ras exhibited *cis-trans* isomerization.

A

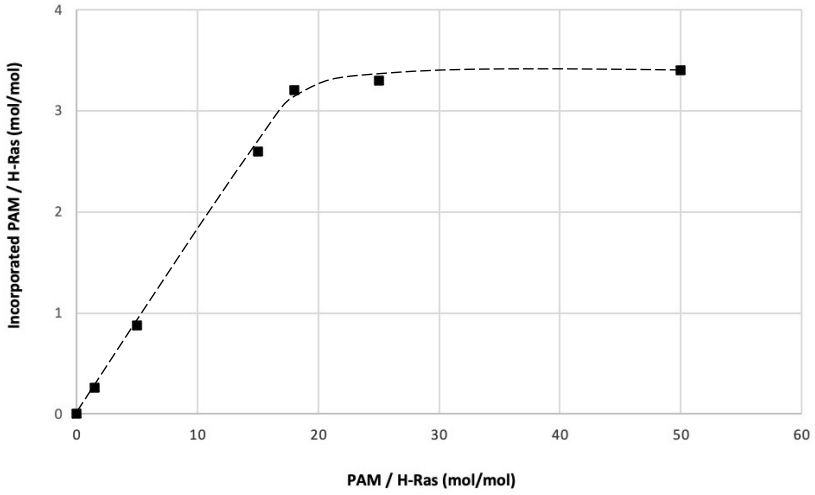

B

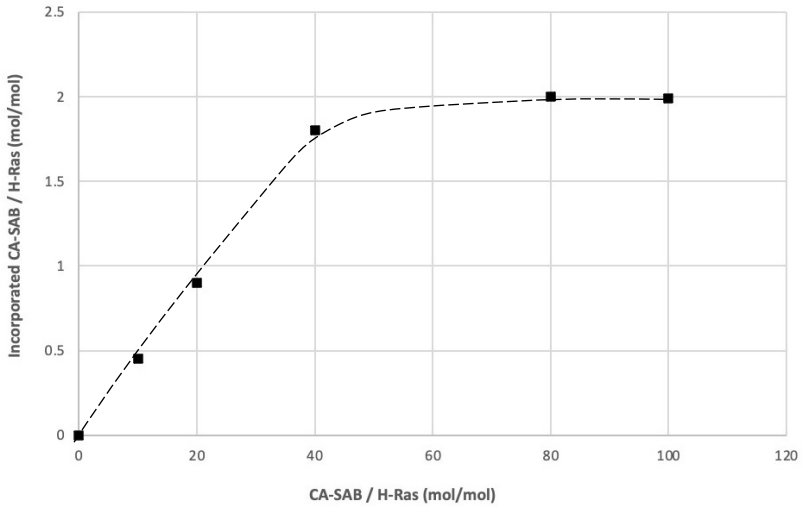

Figure 3. The concentration dependence of azobenzene derivatives incorporation into C118S. (A) H-Ras mutant C118S (5 μM) was reacted with PAM at the concentration of 0, 1.5, 5, 15, 18, 25, and 50 μM for 10 min at 25 °C. (B) H-Ras mutant C118S (5 μM) was reacted with CASAB at the concentration of 0, 10, 20, 40, 80, and 100 μM for 12 h at 25 °C.

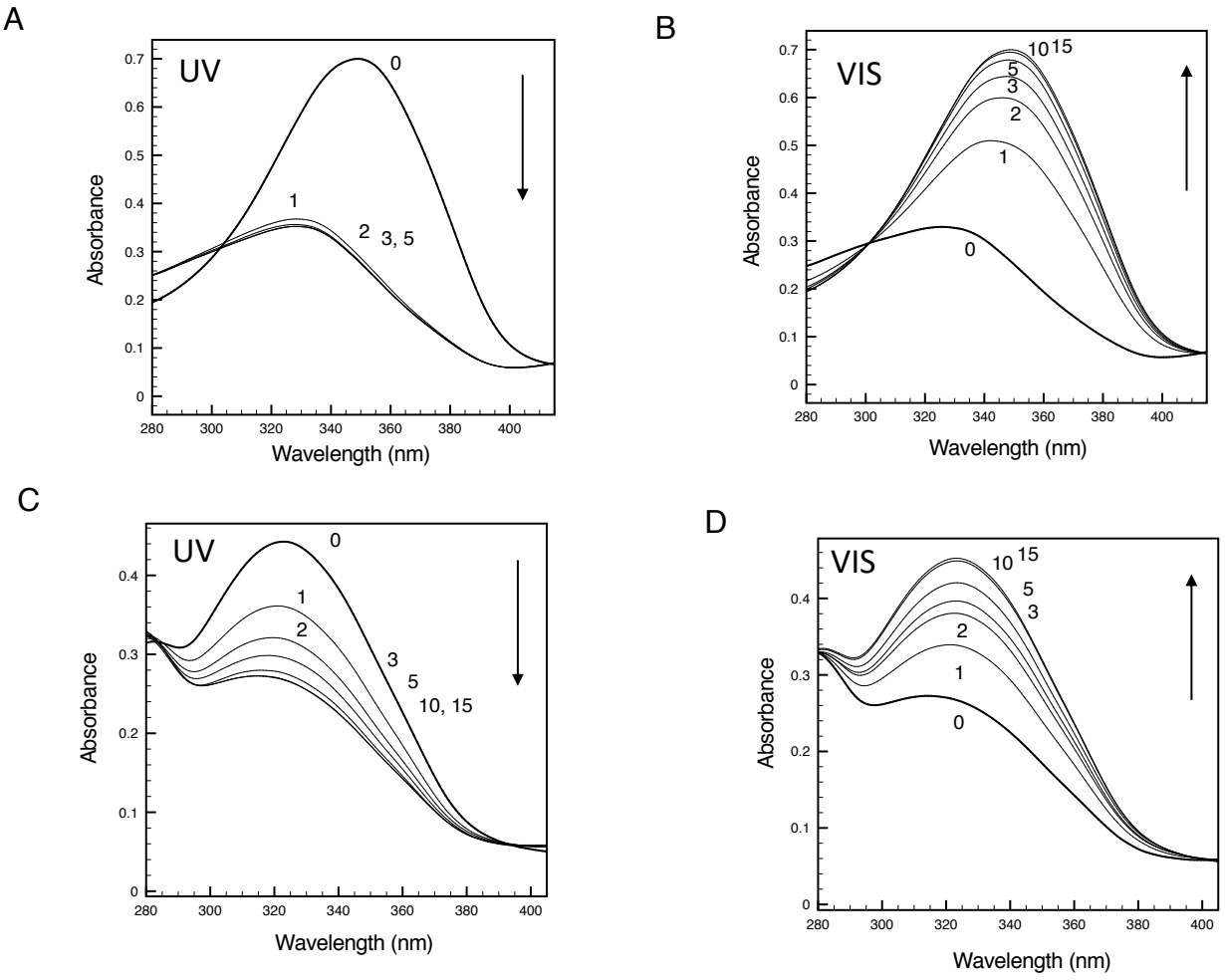

Figure 4. Absorption spectral changes of free PAM and PAM-C118S upon UV and VIS light irradiation. (A) Free PAM was irradiated at 366 nm for 1, 2, 3, and 5 min. (B) Free PAM irradiated at 366 nm for 5 min was subsequently irradiated using fluorescent room light for 1, 2, 3, 5, 10, and 15 min. (C) PAM-C118S was irradiated at 366 nm for 1, 2, 3, 5, 10, and 15 min (D) PAM-C118S irradiated at 366 nm for 5 min was subsequently irradiated using fluorescent room light for 1, 2, 3, 5, 10, and 15 min.

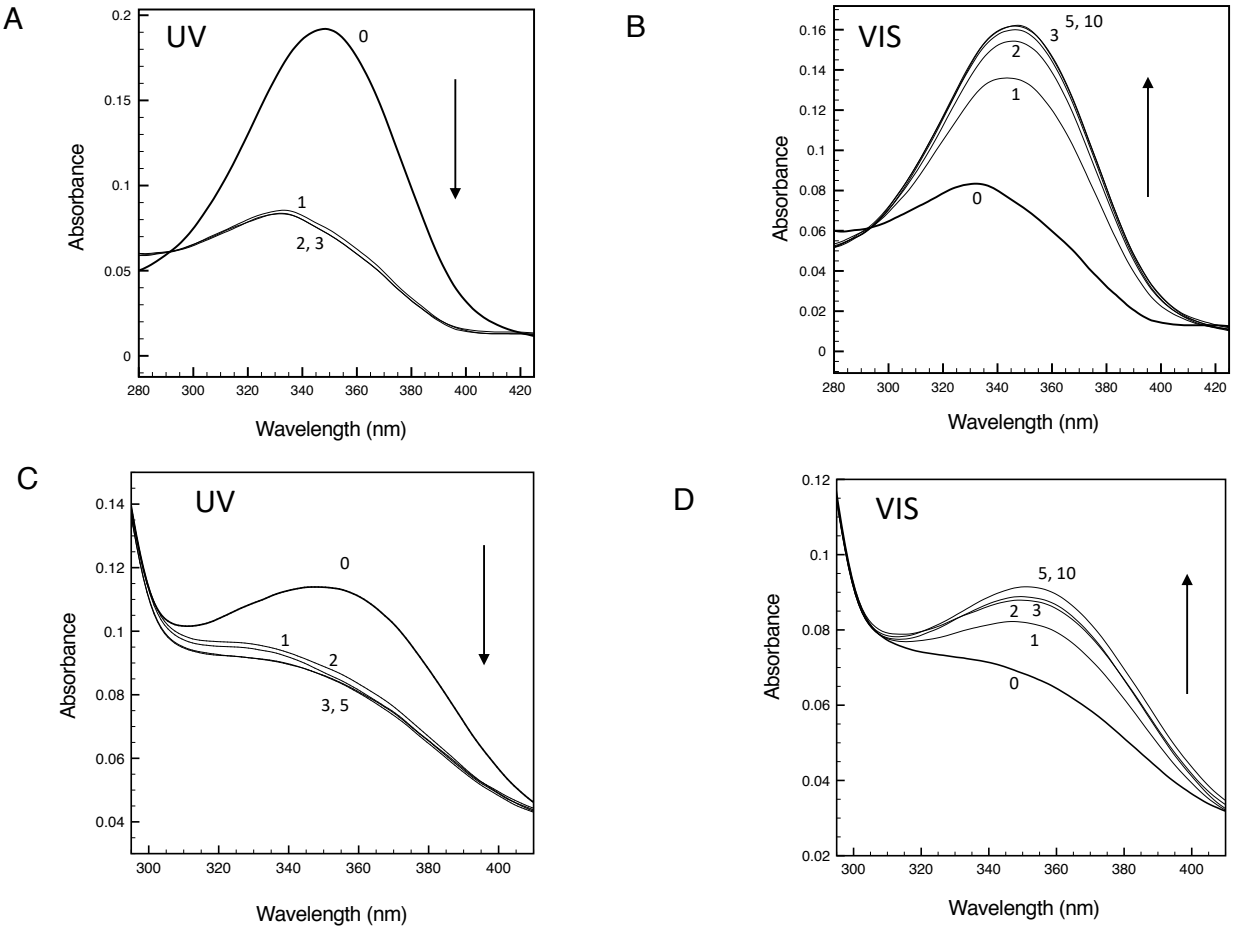

Figure 5. Absorption spectral Changes of free CASAB and CASAB-C118S upon UV and VIS light irradiation. (A) Free CASAB was irradiated at 366 nm for 1, 2, 3, and 5 min. (B) Free CASAB irradiated at 366 nm for 5 min was subsequently irradiated using fluorescent room light for 1, 2, 3, 5, 10, and 15 min. (C) CASAB-C118S was irradiated at 366 nm for 1, 2, 3, and 5 min. (D) CASAB-C118S irradiated at 366 nm for 5 min was subsequently irradiated using fluorescent room light for 1, 2, 3, 5, 10, and 15 min.

Ras GTPase cycle accelerated by GAP and GEF.

Prior to examining the photoregulation of Ras GTPase by modification with photochromic compounds, we established a convenient Ras GTPase assay. It is known that intrinsic Ras GTPase activity is extremely slow to switch to cellular signal transduction. The GTP bound state of Ras behaves as an ON switch, while the GDP bound state behaves as an OFF switch. GTP hydrolysis and export of GDP to GTP were performed by GAP and GEF.

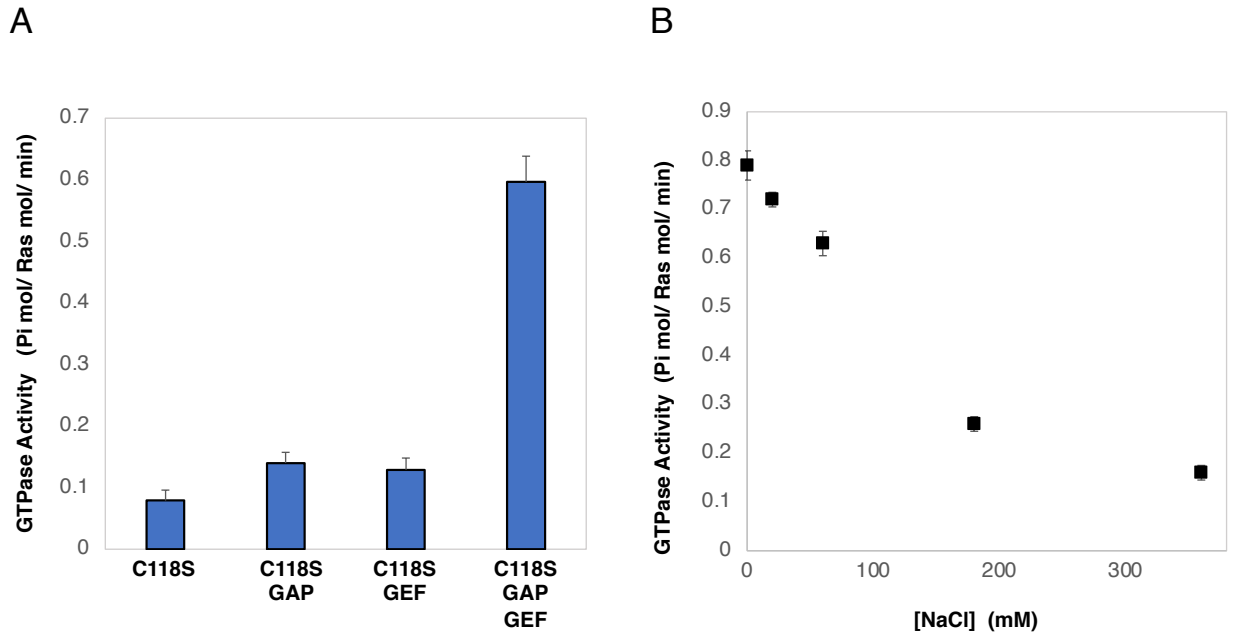

Figure 6. Acceleration of Ras GTPase cycle by GAP and GEF and sodium chloride concentration dependency. (A) The GTPase activity of C118S was assayed in the presence or absence of GAP and GEF. (B) NaCl concentration dependent GTPase activity of C118S was measured with different concentration of NaCl (0, 20, 60, 180, and 360 mM).

It is not easy to show GTP hydrolysis in the catalytic site and monitor the exchange of GDP to GTP due to the requirement of highly sensitive detection methods using radioisotopes. We focused on the acceleration of the GTPase cycle by various factors. Ras cycles GTPase continuously in

the presence of both active regulatory factors. As expected, in the presence of GAP and GEF, the GTPase of C118S was accelerated significantly by approximately 7.5 times, as shown in Figure 6A. Wild-type H-Ras showed almost identical GTPase accelerations (data not shown). GTPase activity was strongly dependent on the concentration of NaCl in the assay buffer (Figure 6B). The GTPase cycle accelerated by GAP and GEF produced sufficient Pi from GTP hydrolysis to be quantified using general Pi detecting reagents.

Photocontrol of Ras GTPase by the isomerization of azobenzene derivatives incorporated into HVR

The effect of isomerization of azobenzene derivatives bound to the HVR of Ras on the GTPase activity in the presence of GAP and GEF has been examined . The transition between *cis* and *trans* isomers of PAM or CASAB on C118S was achieved by UV and visible light irradiation, as described in the Materials and Methods.

GTPase activity of PAM- C118S was changed apparently by UV and Vis light irradiation (Figure 7A). The GTPase activities of *trans*-PAM-C118S and *cis*-PAM-C118S were 70% and 80% of intact C118S, respectively. The differences in GTPase activity between the two isomerization states were not significant but showed reproducibility of photoreversible alteration on the three times of alternate UV and Vis light irradiation. In contrast, CASAB-C118S changed its GTPase activity more significantly than PAM-C118S, accompanied by photoisomerization (Figure 7B). *Trans*-CASAB-C118S reduced the GTPase activity to 62% of intact-C118S. *Cis*-CASAB-C118S exhibited almost the same GTPase activity (95%) as intact C118S. The GTPase activity of CASAB-C118S reversibly was controlled by UV and visible light two times alternate irradiation (Figure 8).

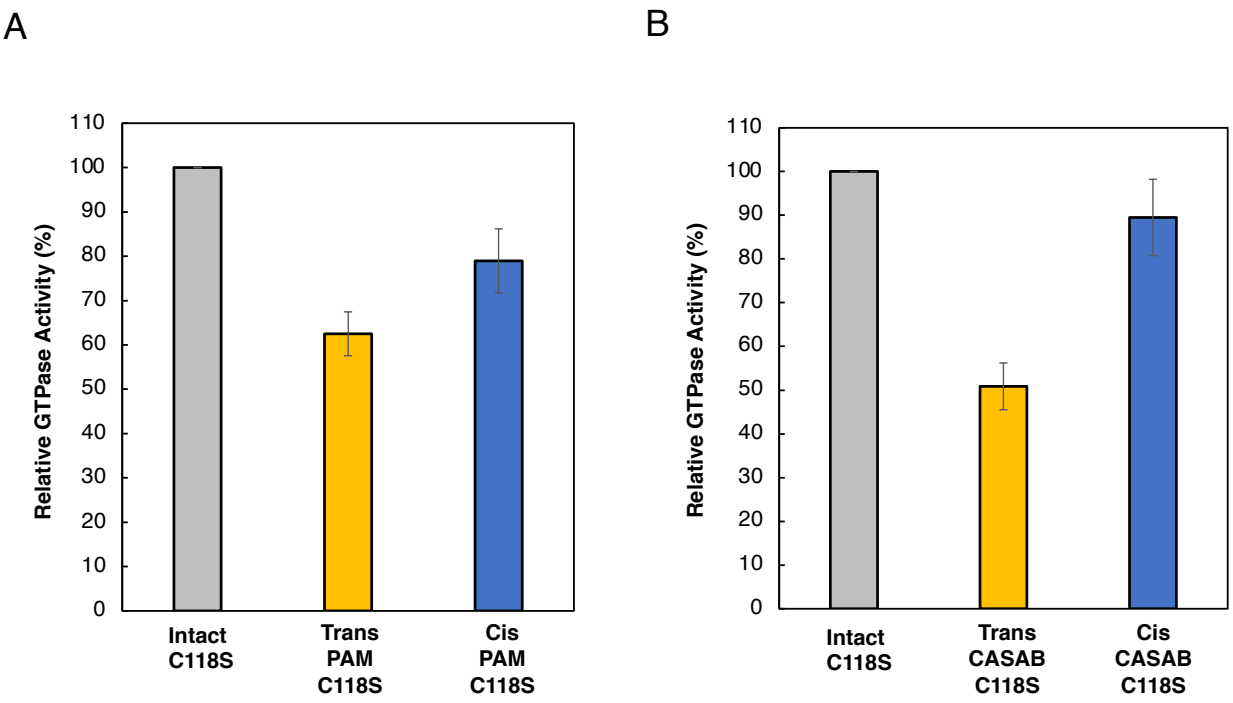

Figure 7. Photocontrol of GTPase activity of the H-Ras (C118S) modified with PAM and CASAB. Prior to ATPase assay, The PAM-C118S and CASAB-C118S were irradiated by UV or VIS light under the same condition described in Figures 4 and 5. The ATPase assay was performed with the same conditions described in the legend for Figure 6A.

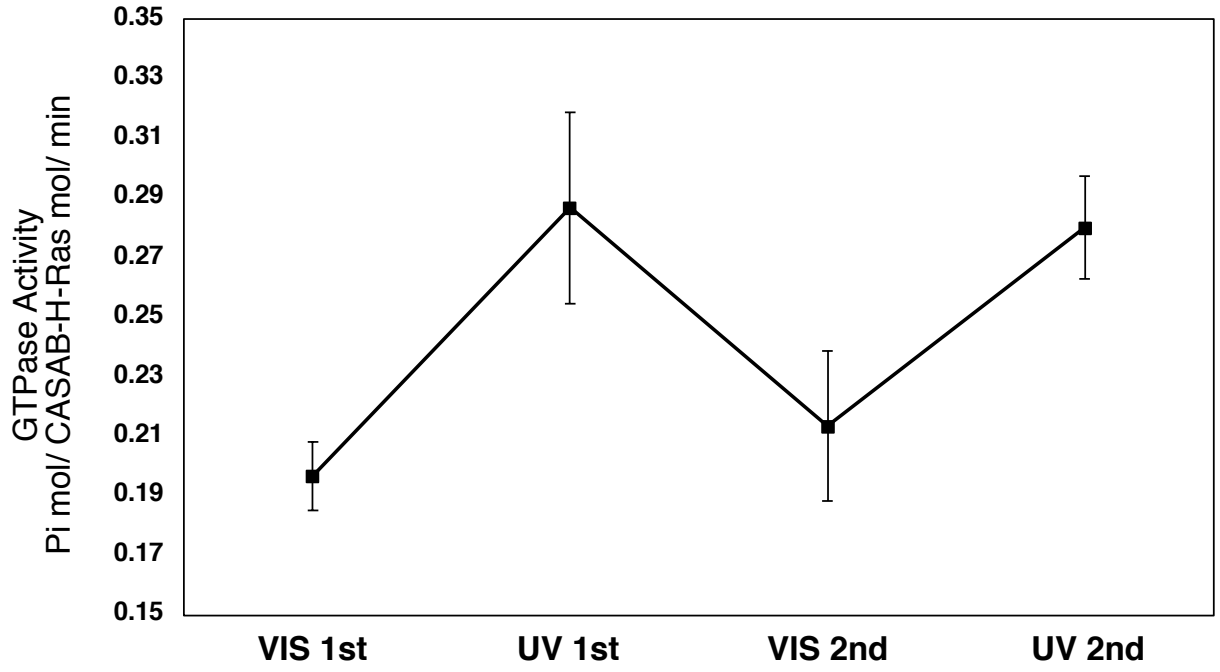

Figure 8. Reproducible reversibility of the alteration of GTPase activity of the C118S modified with CASAB. The CASAB-C118S was irradiated by UV and VIS light alternately and GTPase activity was assayed under the same conditions with Fig. 7. The two times alternating UV–VIS light irradiation was performed.

Formation of H-Ras multimer by modification with azobenzene derivatives and its photocontrol

Previously, we demonstrated that modification of cysteine residues as lipidation sites in HVR with caged compounds induced the formation of Ras multimer, which may mimic the physiological cluster. Therefore, the formation of Ras multimer induced by modification of HVR with PAM and CASAB was also examined by SEC-HPLC according to previously reported methods (11). As shown in Figure 9, intact unmodified H-Ras mutant C118S eluted at approximately 7 min on the SEC-HPLC mentioned in the Materials and Methods section. This elution time was identical to that in our previous report on caged modification (11). On the other hand, PAM C118C showed an elution profile reflecting the formation of the Ras multimer, as we have previously observed on

the caged compound-Ras multimer (11). The peak at 5 min is consistent with the elution of the Ras multimer modified with caged compounds. Moreover, the *cis* isomer of PAM-C118S showed a slightly lower peak than that of the *trans* isomer. These results suggest that the *cis and trans* isomerization of PAM bound to the HVR lipidation sites changes the monomer-multimer equilibrium photoreversibly.

In contrast, small broad peaks were observed at 5 min, while the *cis* and *trans* forms of CASAB-modified H-Ras exhibited almost no multimer formation, as shown in Figure 10. However, apparent differences in the elution profiles around the monomer area were observed between *cis*- and *trans*-CASAB-S118C. The monomer of *trans*-CASAB-S118C exhibited a more widely broadened elution profile. This reflects the conformational differences of HVR in the globular domain between the two isomerization states.

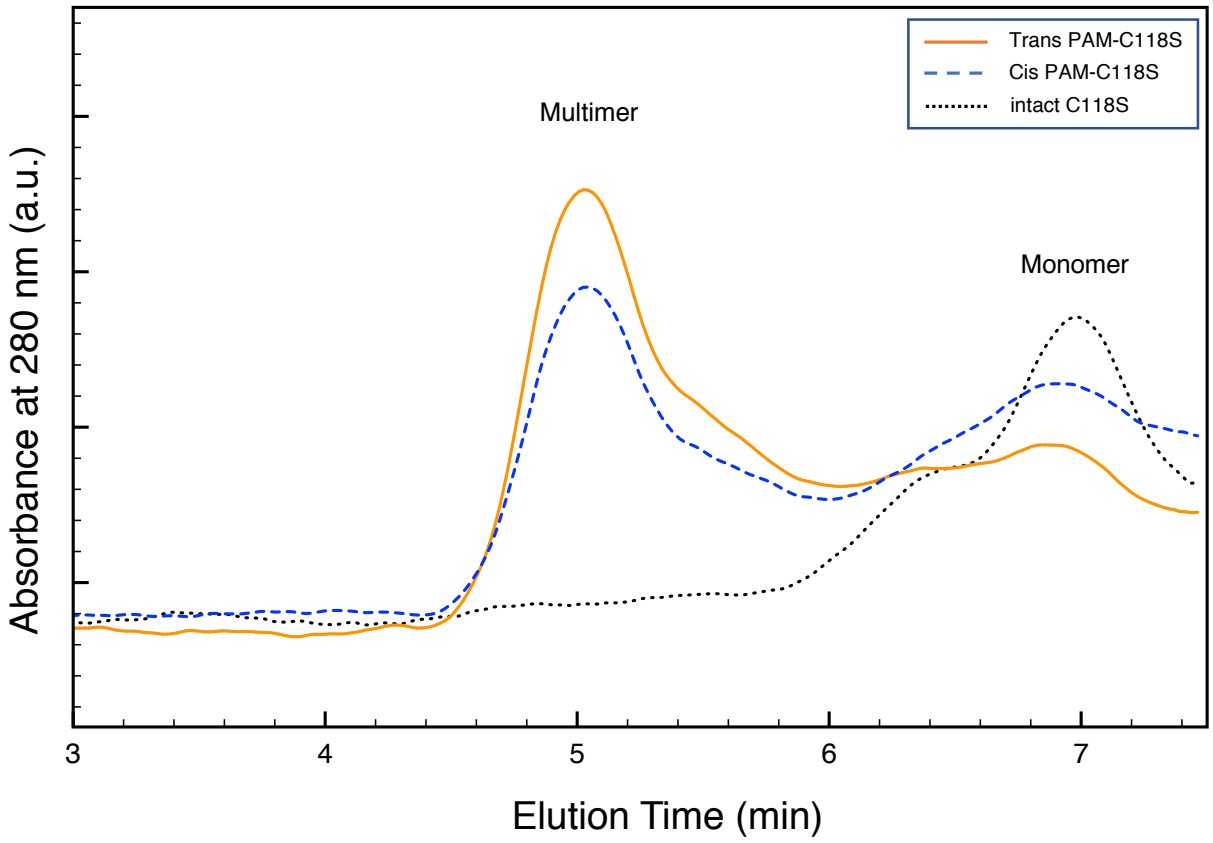

Figure 9. Monitoring the formation H-Ras multimer induced by PAM modification using SEC–HPLC. Elution profile of the C118S modified with PAM. *Trans*-PAM-C118S (broken line), *Cis*-PAM-C118S (black line), and intact C118S (dotted line) were injected into SEC-HPLC (TSKgel G3000PW$_{XL}$ column).

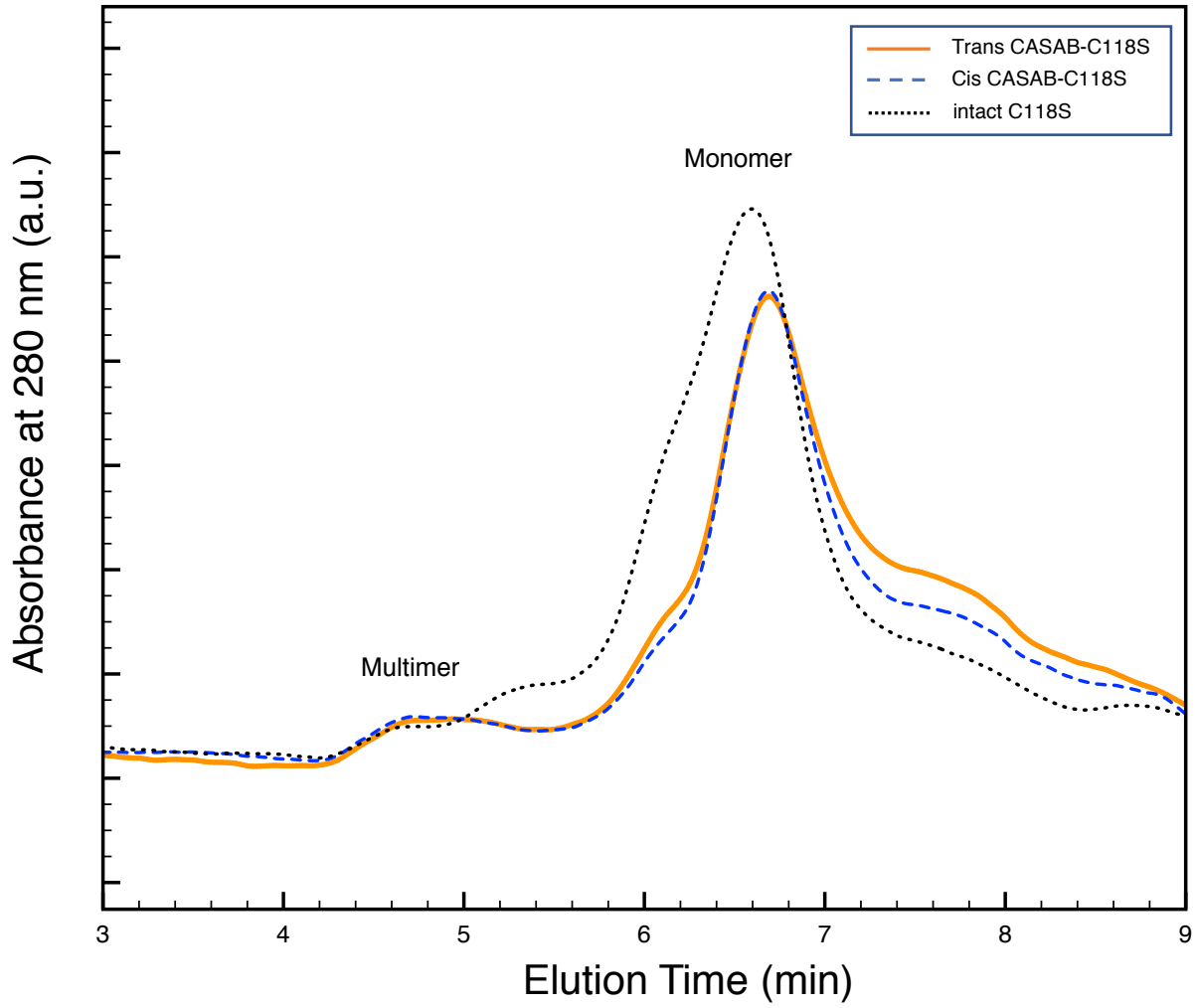

Figure 10. Monitoring the formation H-Ras multimer induced by CASAB modification using SEC–HPLC. Elution profile of the C118S modified with PAM. *Trans*-CASAB-C118S (broken line), *Cis*-CASAB-C118S (black line), and intact C118S (dotted line) were injected into SEC-HPLC (TSKgel G3000PW$_{XL}$ column).

DISCUSSION

The aim of this study is to control the small GTPase Ras, which promotes cellular signal transduction using artificial external stimulus-responsive molecules. Previous crystallographic studies suggested that the GTPase core part of small GTPases comprising Switch I, Switch II, and P-loop is strikingly similar to the ATP driven motor proteins kinesin and myosin (15). Furthermore, structural analysis during the ATPase cycle (16, 17, 18, 19) and the studies of point mutated motor proteins (20, 21) demonstrated the possible mechanical energy transducting system, suggesting that the ATP chemical energy is transmitted to physical-mechanical movement mechanically just like a camshaft motion through rigid domains steric interactions. Therefore, nucleotide-driven functional proteins can be considered as bionanomachines. Furthermore, it is strongly expected that introducing photochromic molecule as an artificial regulatory nanodevice, into the mechanically important sites enables controlling nanomachines. Indeed, we succeeded in photoreversibly controlling motor proteins with an azobenzene derivative incorporated into the key region of energy transducing (22, 23). Subsequently, we have demonstrated that incorporating photochromic compounds into the catalytic domain enables reversible Ras GTPase activity. However, the direct incorporation of photochromic into the catalytic region did not achieve highly efficient reversible control due to direct interaction with the catalytic regions.

In this study, we focused on the regulatory domains of the G protein as a target to incorporate photochromic compounds. HVR is one of the regulatory domains of G protein, which regulates physiological roles.

HVR is the C-terminal region of the G protein and has a unique tail-shaped structure protruding from the catalytic globular domain. The HVR of H-Ras contains three cysteine residues as lipidation sites. Farnesylation and palmitoylation of cysteine residues induce the formation of

dimers or larger multimers as clusters and temporal localization on the plasma membrane. This phenomenon is essential for the cellular signal transduction of G-proteins. Therefore, incorporating photochromic molecules as a photoswitch into HVR is expected to exhibit highly efficient photoreversible regulation of Ras function related to physiological roles.

In support of this idea, Iwata et al. demonstrated that incorporating thiol-reactive caged compounds into HVR lipidation sites induced multimer formation. Subsequently, the multimer returned to the monomer by the elimination reaction of the caged group upon light irradiation. However, the caged compounds exhibited irreversible reactions. Therefore, it does not apply to reversible switching systems.

In the present study, we utilized azobenzene as a photoswitching molecular device for incorporation into the HVR. Azobenzene drastically changes its molecular size and polarity accompanied by *cis*-*trans* isomerization; therefore, it is expected to be a reversible photoswitching of the Ras function.

Two thiol-reactive azobenzene derivatives, PAM and CASAB, were used. PAM, composed of a basic azobenzene moiety and a thiol-reactive maleimide group, is relatively hydrophobic. However, *trans* to *cis* isomerization drastically increases polarity. Therefore, the two isomerization states of PAM are expected to induce different influences on the HVR, which may act as a photoswitching molecular device.

As expected, PAM showed photoregulation of H-Ras GTPase activity, as shown in Figure 7. PAM also induces multimer formation, which may mimic physiological lipidation. Moreover, the *cis* isomer slightly decreased the multimer formation (Figure 9). This may be due to the higher polarity of the cis isomer. Previously, we demonstrated that the formation of the Ras multimer induced by caged compounds strongly depends on the ionic strength (11). A lower concentration of NaCl

induced a modified Ras multimer. Therefore, the driving force to form a multimer is considered to be electrostatic interaction but not hydrophobic interaction of the modified HVR. Modifying HVR with hydrophobic aromatic compounds might induce conformational changes to open the electrostatic intermolecular interaction sites on the globular domain of H-Ras. The *cis* and *trans* isomers of PAM change the HVR conformation to induce slightly different states of the globular domain to interact intermolecularly, resulting in different efficient multimer formations. On the other hand, H-Ras modified with CASAB did not form multimers, as shown in Figure 10. CASAB contains a highly negatively charged sulfonate group, which is completely opposite to hydrophobic lipidation. Therefore, modification with CASAB might not induce conformational changes to form multimers that mimic physiological clusters. However, although CASAB-H-Ras did not exhibit multimer formation, the GTPase activity of CASAB-H-Ras was photo-controlled by *cis and trans* isomerization by UV and visible light irradiation more efficiently than that of PAM-H-Ras. As azobenzene drastically changes its structure by *cis* and *trans* isomerization (24, 25), the sulfonate moiety in CASAB changes its location on the HVR. Therefore, it is considered that the *trans* isomer moves the position of the sulfonate group to interfere with the GAP or GEF interaction with H-Ras, resulting in a lower GTPase. The *cis*-isomer exhibited almost normal GTPase activity (Figure 7B).

CONCLUSION

We have successfully demonstrated that incorporating thiol-reactive photochromic azobenzene derivatives into the lipidation site in HVR, which is one of the physiologically functional sites of H-Ras, enables the reversible control of GTPase activity and multimer formation by UV and visible light irradiation. The technique utilizing photochromic molecular devices may be applicable to other functional molecules as bionanomachines. The further studies on this research field are expected to contribute to the development of photo-regulated functional biomolecules which have physiologically important roles.

CHAPTER 4

OVERALL SUMMARY:

Structural analysis of H-Ras multimer by Electron microscopic method reveals the disk shape and pentamer formation which is consistent with one of the possible structures estimated from the data of small angle X-ray scattering indicating physiological conformational changes of HVR domain during lipidation. Another approach to regulate the function of Ras using azobenzene derivatives incorporating into the HVR domain showed successful photoregulation. That can be possible application to control the ras function which is involved into the cancer formation.

REFERENCES

CHAPTER 1

1. Tuteja, N. (2009). Signaling through G protein coupled receptors. Plant signaling & behavior, 4(10), 942-947.

2. Karchin, R., Karplus, K., & Haussler, D. (2002). Classifying G-protein coupled receptors with support vector machines. Bioinformatics, 18(1), 147-159.

3. Kobilka, B. (1992). Adrenergic receptors as models for G protein-coupled receptors. Annual review of neuroscience, 15(1), 87-114.

4. Guo, Y. Z., Li, M., Lu, M., Wen, Z., Wang, K., Li, G., & Wu, J. (2006). Classifying G protein-coupled receptors and nuclear receptors on the basis of protein power spectrum from fast Fourier transform. Amino Acids, 30(4), 397-402.

5. Han, C. W., Jeong, M. S., & Jang, S. B. (2017). Structure, signaling and the drug discovery of the Ras oncogene protein. BMB reports, 50(7), 355–360. https://doi.org/10.5483/bmbrep.2017.50.7.062

6. Ye, X., & Carew, T. J. (2010). Small G protein signaling in neuronal plasticity and memory formation: the specific role of ras family proteins. Neuron, 68(3), 340-361.

7. Schmitt, J. M., & Stork, P. J. (2001). Cyclic AMP-mediated inhibition of cell growth requires the small G protein Rap1. Molecular and cellular biology, 21(11), 3671-3683.

8. Broder, Y. C., Katz, S., & Aronheim, A. (1998). The ras recruitment system, a novel approach to the study of protein–protein interactions. Current Biology, 8(20), 1121-1130.

9. Matozaki, T., Nakanishi, H., & Takai, Y. (2000). Small G-protein networks:: Their crosstalk and signal cascades. Cellular signalling, 12(8), 515-524.

10. Nobes, C., & Hall, A. (1994). Regulation and function of the Rho subfamily of small GTPases. Current opinion in genetics & development, 4(1), 77-81.

11. Spiering, D., & Hodgson, L. (2011). Dynamics of the Rho-family small GTPases in actin regulation and motility. Cell adhesion & migration, 5(2), 170-180.

12. Braga, V. M., Machesky, L. M., Hall, A., & Hotchin, N. A. (1997). The small GTPases Rho and Rac are required for the establishment of cadherin-dependent cell–cell contacts. The Journal of cell biology, 137(6), 1421-1431.

13. Valencia, A., Chardin, P., Wittinghofer, A., & Sander, C. (1991). The ras protein family: evolutionary tree and role of conserved amino acids. Biochemistry, 30(19), 4637-4648.

14. Drivas, G. T., Palmieri, S., D'Eustachio, P., & Rush, M. G. (1991). Evolutionary grouping of the RAS-protein family. Biochemical and biophysical research communications, 176(3), 1130-1135.

15. Rojas, A. M., Fuentes, G., Rausell, A., & Valencia, A. (2012). The Ras protein superfamily: evolutionary tree and role of conserved amino acids. Journal of Cell Biology, 196(2), 189-201.

16. Finlin, B. S., & Andres, D. A. (1997). Rem is a new member of the Rad-and Gem/Kir Ras-related GTP-binding protein family repressed by lipopolysaccharide stimulation. Journal of Biological Chemistry, 272(35), 21982-21988.

17. Wittinghofer, A., & Pal, E. F. (1991). The structure of Ras protein: a model for a universal molecular switch. Trends in biochemical sciences, 16, 382-387.

18. Feig, L. A., & Cooper, G. M. (1988). Inhibition of NIH 3T3 cell proliferation by a mutant ras protein with preferential affinity for GDP. Molecular and cellular biology, 8(8), 3235-3243.

19. Rowinsky, E. K., Windle, J. J., & Von Hoff, D. D. (1999). Ras protein farnesyltransferase: a strategic target for anticancer therapeutic development. Journal of Clinical Oncology, 17(11), 3631-3652.

20. Riely, G. J., Marks, J., & Pao, W. (2009). KRAS mutations in non–small cell lung cancer. Proceedings of the American Thoracic Society, 6(2), 201-205.

21. Riely, G. J., Marks, J., & Pao, W. (2009). KRAS mutations in non–small cell lung cancer. Proceedings of the American Thoracic Society, 6(2), 201-205.

22. Misale, S., Yaeger, R., Hobor, S., Scala, E., Janakiraman, M., Liska, D., ... & Bardelli, A. (2012). Emergence of KRAS mutations and acquired resistance to anti-EGFR therapy in colorectal cancer. Nature, 486(7404), 532-536.

23. Cooper, G. M., & Hausman, R. O. B. E. R. T. E. (2000). A molecular approach. The Cell. 2nd ed. Sunderland, MA: Sinauer Associates.

24. Engelhardt, W. A., & Ljubimowa, M. N. (2013). Myosine and adenosinetriphosphatase. In A Source Book in Chemistry, 1900-1950 (pp. 378-381). Harvard University Press.

25. Cafiero, M. (1950). Adenosine triphosphatase and myosine in the embryo chick during development. Bollettino della Societa italiana di biologia sperimentale, 26, 512-513.

26. Bos, J. L., Rehmann, H., & Wittinghofer, A. (2007). GEFs and GAPs: critical elements in the control of small G proteins. Cell, 129(5), 865-877.

27. Cherfils, J., & Zeghouf, M. (2013). Regulation of small gtpases by gefs, gaps, and gdis. Physiological reviews, 93(1), 269-309.

28. Ahmad, K. F., & Lim, W. A. (2010). The minimal autoinhibited unit of the guanine nucleotide exchange factor intersectin. PLoS One, 5(6), e11291.

29. Amor, J. C., Swails, J., Zhu, X., Roy, C. R., Nagai, H., Ingmundson, A., ... & Kahn, R. A. (2005). The structure of RalF, an ADP-ribosylation factor guanine nucleotide exchange factor from Legionella pneumophila, reveals the presence of a cap over the active site. Journal of Biological Chemistry, 280(2), 1392-1400.

30. Barlowe, C., & Schekman, R. (1993). SEC12 encodes a guanine-nucleotide-exchange factor essential for transport vesicle budding from the ER. Nature, 365(6444), 347-349.

31. Barr, F., & Lambright, D. G. (2010). Rab gefs and gaps. Current opinion in cell biology, 22(4), 461-470.

32. Cronin, T. C., DiNitto, J. P., Czech, M. P., & Lambright, D. G. (2004). Structural determinants of phosphoinositide selectivity in splice variants of Grp1 family PH domains. The EMBO journal, 23(19), 3711-3720.

33. Durr, H., & Bouas-Laurent, H. (Eds.). (2003). Photochromism: molecules and systems. Elsevier.

34. Exelby, R., & Grinter, R. (1965). Phototropy (or photochromism). Chemical Reviews, 65(2), 247-260.

35. Irie, M. (2000). Photochromism: memories and switches introduction. Chemical Reviews, 100(5), 1683-1684.

36. Gust, D., Andréasson, J., Pischel, U., Moore, T. A., & Moore, A. L. (2012). Data and signal processing using photochromic molecules. Chemical Communications, 48(14), 1947-1957.

37. Nahar, R., Iwata, S., Morita, D., Tahara, Y., Sugimoto, Y., Miyata, M., & Maruta, S. (2021). Multimerization of Small G-protein H-Ras Induced by Chemical Modification at Hyper Variable Region with Caged Compound. The Journal of Biochemistry.

38. Tsujioka, T., & Irie, M. (2010). Electrical functions of photochromic molecules. Journal of Photochemistry and Photobiology C: Photochemistry Reviews, 11(1), 1-14.

39. Parrot, A., Izzet, G., Chamoreau, L. M., Proust, A., Oms, O., Dolbecq, A., ... & Mialane, P. (2013). Photochromic properties of polyoxotungstates with grafted spiropyran molecules. Inorganic chemistry, 52(19), 11156-11163.

CHAPTER 2

1. Fernández-Medarde, A., and Santos, E. (2011) Ras in cancer and developmental diseases. Genes Cancer 2, 344–358.

2. Campbell, S. L., Khosravi-Far, R., Rossman, K. L., Clark, G. J., and Der, C. J. (1998) Increasing complexity of Ras signaling. Oncogene 17, 1395–1413.

3. Rajalingam, K., Schreck, R., Rapp, U. R., and Albert, S. (2007) Ras oncogenes and their downstream targets. Biochim. Biophys. Acta 1773, 1177–1195.

4. Weise, K., Kapoor, S., Denter, C., Nikolaus, J., Opitz, N., Koch, S., Triola, G., Herrmann, A., Waldmann, H., and Winter, R. (2011) Membrane-mediated induction and sorting of K-Ras microdomain signaling platforms. J. Am. Chem. Soc. 133, 880–887.

5. Inouye, K., Mizutani, S., Koide, H., and Kaziro, Y. (2000) Formation of the Ras Dimer Is Essential for Raf-1 Activation. J. Biol. Chem. 275, 3737–3740.

6. Kozielski, F., Sack, S., Marx, a., Thormählen, M., Schönbrunn, E., Biou, V., Thompson, a., Mandelkow, E. M., and Mandelkow, E. (1997) The crystal structure of dimeric kinesin and implications for microtubule-dependent motility. Cell 91, 985–994.

7. Scholey, J. E., Nithianantham, S., Scholey, J. M., and Al-Bassam, J. (2014) Structural basis for the assembly of the mitotic motor Kinesin-5 into bipolar tetramers. Elife 3, 1–19.

8. Chène, P. (2001) The role of tetramerization in p53 function. Oncogene 20, 2611–2617.

9. Klumpp, M., Baumeister, W., and Essen, L.-O. (1997) Structure of the Substrate Binding Domain of the Thermosome, an Archaeal Group II Chaperonin. Cell 91, 263–270.

10. Marchetti, A., Parker, M. S., Moccia, L. P., Lin, E. O., Arrieta, A. L., Ribalet, F., Murphy, M. E. P., Maldonado, M. T., and Armbrust, E. V. (2009) Ferritin is used for iron storage in bloom-forming marine pennate diatoms. Nature 457, 467–470.

11. Ellis-Davies, G. C. R. (2007) Caged compounds: photorelease technology for control of cellular chemistry and physiology. Nat. Methods 4, 619–628.

12. Tani, T., and Kamimura, S. (1999) Dynein-ADP as a force-generating intermediate revealed by a rapid reactivation of flagellar axoneme. Biophys. J. 77, 1518–1527.

13. Dantzig, J. A., Higuchi, H., and Goldman, Y. E. (1998) Studies of molecular motors using caged compounds. Methods Enzymol. 291, 307–348.

14. Ellis-Davies, G. C. R. (1998) Synthesis of photosensitive EGTA derivatives. Tetrahedron Lett. 39, 953–956.

15. Trigo, F. F., Bouhours, B., Rostaing, P., Papageorgiou, G., Corrie, J. E. T., Triller, A., Ogden, D., and Marty, A. (2010) Presynaptic miniature GABAergic currents in developing interneurons. Neuron 66, 235–247.

16. Ohmuro-Matsuyama, Y., and Tatsu, Y. (2008) Photocontrolled cell adhesion on a surface functionalized with a caged arginine-glycine-aspartate peptide. Angew. Chem. Int. Ed. Engl. 47, 7527–7529.

17. Chou, C., and Deiters, A. (2011) Light-Activated Gene Editing with a Photocaged Zinc-Finger Nuclease. Angew. Chemie Int. Ed. 50, 6839–6842.

18. Givens, R. S., Weber, J. F., Jung, A. H., and Park, C. H. (1998) New photoprotecting groups: desyl and p-hydroxyphenacyl phosphate and carboxylate esters. Methods Enzymol. 291, 1–29.

19. Chang, C., Fernandez, T., Panchal, R., and Bayley, H. (1998) Caged Catalytic Subunit of cAMP-Dependent Protein Kinase. J. Am. Chem. Soc. 120, 7661–7662.

20. Lawrence, D. S. (2005) The preparation and in vivo applications of caged peptides and proteins. Curr. Opin. Chem. Biol. 9, 570–575.

21. Pan, P., and Bayley, H. (1997) Caged cysteine and thiophosphoryl peptides. FEBS Lett. 405, 81–85.

22. Marriott, G., and Heidecker, M. (1996) Light-directed generation of the actin-activated ATPase activity of caged heavy meromyosin. Biochemistry 35, 3170–3174.

23. A.P.Hammersley, (1997) FIT2D: An Introduction and Overview. ESRF Internal Report.

24. ESRF97HA02T Konarev, P. V, Volkov, V. V, Sokolova, A. V, Koch, M. H. J., and Svergun, D. I. (2003) PRIMUS : a Windows PC-based system for small-angle scattering data analysis. J. Appl. Crystallogr. 36, 1277–1282.

25. P.V.Konarev, V.V.Volkov, A.V.Sokolova, M.H.J.Koch and D. I. Svergun (2003). PRIMUS - a Windows-PC based system for small-angle scattering data analysis. J Appl Cryst. 36, 1277-1282.

26. Franke, D. and Svergun, D.I. (2009) DAMMIF, a program for rapid ab-initio shape determination in small-angle scattering. J. Appl. Cryst., 42, 342-346

27. Katayama, E., & Ikebe, M. (1995). Mode of caldesmon binding to smooth muscle thin filament: possible projection of the amino-terminal of caldesmon from native thin filament. Biophysical journal, 68(6), 2419–2428.

28. Sarkar-Banerjee, S., Sayyed-Ahmad, A., Prakash, P., Cho, K. J., Waxham, M. N., Hancock, J. F., & Gorfe, A. A. (2017). Spatiotemporal analysis of K-Ras plasma membrane interactions reveals multiple high order homo-oligomeric complexes. Journal of the American Chemical Society, 139(38), 13466-13475.

29. Plowman, S. J., Ariotti, N., Goodall, A., Parton, R. G., & Hancock, J. F. (2008). Electrostatic interactions positively regulate K-Ras nanocluster formation and function. Molecular and cellular biology, 28(13), 4377-4385.

30. Zhou, Y., & Hancock, J. F. (2015). Ras nanoclusters: Versatile lipid-based signaling platforms. Biochimica et Biophysica Acta (BBA)-Molecular Cell Research, 1853(4), 841-849.

31. Abankwa, D., Hanzal-Bayer, M., Ariotti, N., Plowman, S. J., Gorfe, A. A., Parton, R. G., ... & Hancock, J. F. (2008). A novel switch region regulates H-ras membrane orientation and signal output. The EMBO journal, 27(5), 727-735.

32. Abankwa, D., Gorfe, A. A., & Hancock, J. F. (2008). Mechanisms of Ras membrane organization and signalling: Ras on a rocker. Cell cycle (Georgetown, Tex.), 7(17), 2667–2673.

33. Yang, M.H., Nickerson, S., Kim, E.T., Liot, C., Laurent, G., Spang, R., Philips, M.R., Shan, Y., Shaw, D.E., Bar-Sagi, D., Haigis, M.C., and Haigis, K.M. (2012) Regulation of Ras oncogenicity by acetylation. Proc. Natl. Acad. Sci. USA 109, 10843–10848

CHAPTER 3

1. Fernandez-Medarde, A., & Santos, E. (2011). Ras in cancer and developmental diseases. Genes Cancer 2: 344–358.

2. Campbell, S. L., Khosravi-Far, R., Rossman, K. L., Clark, G. J., & Der, C. J. (1998). Increasing complexity of Ras signaling. Oncogene, 17(11), 1395-1413.

3. Marshall, C. B., Meiri, D., Smith, M. J., Mazhab-Jafari, M. T., Gasmi-Seabrook, G. M., Rottapel, R., ... & Ikura, M. (2012). Probing the GTPase cycle with real-time NMR: GAP and GEF activities in cell extracts. Methods, 57(4), 473-485.

4. Kull, F. J., Vale, R. D., & Fletterick, R. J. (1998). The case for a common ancestor: kinesin and myosin motor proteins and G proteins. Journal of Muscle Research & Cell Motility, 19(8), 877-886.

5. Yamada, M. D., Nakajima, Y., Maeda, H., & Maruta, S. (2007). Photocontrol of kinesin ATPase activity using an azobenzene derivative. Journal of biochemistry, 142(6), 691-698.

6. Sadakane, K., Alrazi, I. M., & Maruta, S. (2018). Highly efficient photocontrol of mitotic kinesin Eg5 ATPase activity using a novel photochromic compound composed of two azobenzene derivatives. The Journal of Biochemistry, 164(4), 295-301.

7. Alrazi, I. M., Sadakane, K., & Maruta, S. (2021). Novel photochromic inhibitor for mitotic kinesin Eg5 which forms multiple isomerization states. The Journal of Biochemistry.

8. Iwata, S., & Maruta, S. (2015). Photocontrol of the GTPase activity of the small G protein K-Ras by using an azobenzene derivative. Biochemistry and biophysics reports, 4, 268-276.

9. Nussinov, R., Tsai, C. J., & Jang, H. (2019, February). Is Nanoclustering essential for all oncogenic KRas pathways? Can it explain why wild-type KRas can inhibit its oncogenic variant?. In Seminars in cancer biology (Vol. 54, pp. 114-120). Academic Press.

10. Rotblat, B., Belanis, L., Liang, H., Haklai, R., Elad-Zefadia, G., Hancock, J. F., ... & Plowman, S. J. (2010). H-Ras nanocluster stability regulates the magnitude of MAPK signal output. PloS one, 5(8), e11991.

11. Nahar, R. (2021). Structural Analysis of Small G-Protein Ras Multimer Induced by Chemical Modification of HVR Domain with Caged Compound. Biophysical Journal, 120(3), 295a.

12. Ellis-Davies, G. C. (2020). Useful caged compounds for cell physiology. Accounts of Chemical Research, 53(8), 1593-1604.)

13. Shishido, H., Yamada, M. D., Kondo, K., & Maruta, S. (2009). Photocontrol of calmodulin interaction with target peptides using azobenzene derivative. Journal of biochemistry, 146(4), 581–590.

14. Rau, H. (2002). Photoisomerization of azobenzenes. Photoreactive Organic Thin Films, 3-47.

15. Kull, F. J., Vale, R. D., & Fletterick, R. J. (1998). The case for a common ancestor: kinesin and myosin motor proteins and G proteins. Journal of Muscle Research & Cell Motility, 19(8), 877-886.

16. Kull, F. J., Sablin, E. P., Lau, R., Fletterick, R. J., & Vale, R. D. (1996). Crystal structure of the kinesin motor domain reveals a structural similarity to myosin. Nature, 380(6574), 550-555.

17. Rayment, I., Rypniewski, W. R., Schmidt-Base, K., Smith, R., Tomchick, D. R., Benning, M. M., ... & Holden, H. M. (1993). Three-dimensional structure of myosin subfragment-1: a molecular motor. Science, 261(5117), 50-58.

18. Fisher, A. J., Smith, C. A., Thoden, J., Smith, R., Sutoh, K., Holden, H. M., & Rayment, I. (1995). X-ray structures of the myosin motor domain of dictyostelium discoideum complexed with MgADP. cntdot. BeFx and MgADP. cntdot. AlF4. Biochemistry, 34(28), 8960-8972.

19. Dominguez, R., Freyzon, Y., Trybus, K. M., & Cohen, C. (1998). Crystal structure of a vertebrate smooth muscle myosin motor domain and its complex with the essential light chain: Visualization of the pre–power stroke state. Cell, 94(5), 559-571.

20. Klumpp, L. M., Brendza, K. M., Gatial, J. E., Hoenger, A., Saxton, W. M., & Gilbert, S. P. (2004). Microtubule− kinesin interface mutants reveal a site critical for communication. Biochemistry, 43(10), 2792-2803.

21. Yun, M., Zhang, X., Park, C. G., Park, H. W., & Endow, S. A. (2001). A structural pathway for activation of the kinesin motor ATPase. The EMBO Journal, 20(11), 2611-2618.

22. Umeki, N., Yoshizawa, T., Sugimoto, Y., Mitsui, T., Wakabayashi, K., & Maruta, S. (2004). Incorporation of an azobenzene derivative into the energy transducing site of skeletal muscle myosin results in photo-induced conformational changes. Journal of biochemistry, 136(6), 839-846.

23. Ishikawa, K., Tamura, Y., & Maruta, S. (2014). Photocontrol of mitotic kinesin Eg5 facilitated by thiol-reactive photochromic molecules incorporated into the loop L5 functional loop. The Journal of Biochemistry, 155(3), 195-206.

24. Timpe, H. J. (1991). Photochromism–molecules and systems. Herausgeber: Dürr, H., Bouas-Laurent, H. 1. Auflage, 1068 S. Amsterdam, Oxford, New York, Tokyo: Elsevier, 1990. Schriftenreihe: Studies in organic chemistry, 40. ISBN 0-444-87432-1.

25. Beharry, A. A., & Woolley, G. A. (2011). Azobenzene photoswitches for biomolecules. Chemical Society Reviews, 40(8), 4422-4437.

Acknowledgement

I cannot express enough thanks to my supervisor Dr. Shinsaku Maruta and lab members for their continued support and encouragement. My collaborators from Nagoya University, Osaka City University, Japan, I offer my sincere appreciation for the learning opportunities provided by my Collaborators.

Finally, to my caring, loving and supportive family, my deepest gratitude. Their encouragement when the times got rough are much appreciated and duly noted.